Durham E-Theses

Some electrical properties of lithium sialons

Sally K. Kavanagh

How to cite:

Use policy

SOME ELECTRICAL PROPERTIES

OF LITHIUM SIALONS

by

SALLY K. KAVANAGH, B.Sc.

A thesis submitted to the Faculty of Science of the

University of Durham for the Degree of Master of Science

Department of Applied Physics
and Electronics
Science Laboratories
Durham City

April 1977

ABSTRACT

Sialons are a new range of high strength, refractory materials which can be prepared by hot-pressing mixtures of silicon nitride (Si_3N_4) and alumina (Al_2O_3) at temperatures of about 1700°C. The resulting ceramics have a general formula

$$Si_{6-z}Al_zO_zN_{8-z}$$
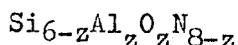
where z may vary from 3 to 4. Their crystal structure is similar to that of Si_3N_4 but N^{3-} is replaced by O^{2-} and, to effect charge compensation, Si^{4+} is replaced by Al^{3+}. Charge compensation can also be achieved by **introducing** other metal ions such as Li^+, Na^+, Mg^{2+} and Y^{3+}. This leads to an even greater possible range of ceramics. The present work is concerned with one group of these, the lithium sialons.

The small amount of previous work on the electrical properties of lithium sialons was confined to preliminary measurements of d.c. conductivity. Here the electrical behaviour of a range of lithium sialons has been studied and then compared with that of pure sialons and an yttrium sialon glass in order to determine the conductivity mechanism operating within the lithium sialon samples.

The orders of magnitude of conductivity encountered lay between $10^{-7}(\text{ohm cm})^{-1}$ and $10^{-3}(\text{ohm cm})^{-1}$. Techniques have been developed for the measurement of d.c. conductivity (σ_{dc}) from room temperature to 800°C and of a.c. conductivity (σ_{ac}) from 20 Hz to 25 kHz over the same temperature range. The measurements also enabled dielectric constant and losses to be determined at the same temperatures and frequencies. The results showed the presence of two conductivity regimes, one above and one below about 400°C. It has also been

observed that σ_{dc} decreases as a result of passing current through the specimen and a preliminary examination of this apparent solid state electrolysis has been made. All the results are discussed in comparison with the available data on pure sialons and some other nitrogen ceramics.

CONTENTS

CHAPTER 1

INTRODUCTION

1-1 The Nature of Ceramics

The materials which were described by the Greek word "keramos" meaning burnt stuff, have mushroomed into a ceramics industry which now manufactures materials essential for almost every realm of life as we know it.

Traditional ceramics are those based on the silicate structure and include porcelain, pottery, cements and glasses. In common with all ceramics they are predominantly co-valently bonded, inorganic and non-metallic. Many of them are also characterised by extremely high melting points and have an excellent resistance to chemical attack. In the last two decades the ceramics field has broadened considerably and has developed new or "Special Ceramics" in response to the demand from modern technology for ever greater efficiency and the higher operating temperatures associated with it.

Many of these special ceramics have been found to display novel properties which have proved imperative to many newer fields of technology. The space and computer industries are two good examples. Magnetic ceramics have been developed for use in electronic memory circuits. For this application an almost square hysteresis loop is required which the special ceramics have been able to offer. In missile and rocket development the nose cone and rocket throat must be able to withstand extreme temperatures and display good erosion resistance. Ceramics are now used for both. It is interesting that in the generation of nuclear power, ceramic fuels based on urania have proved invaluable.

One of the most ineresting potential uses of special ceramics is in the development of gas turbine engines. It is proposed to

use one such ceramic, silicon nitride, to manufacture the blades in these engines which would enable the operating temperature to be raised to 1350°C. This would represent a worthwhile increase in efficiency.

Silicon nitride has been hailed as the ceramic of the decade many times. Its properties are truly remarkable. It decomposes at 1950°C but it can be used up to 1870°C in an atmosphere of helium or hydrogen. It is oxidation resistant in air up to 1500°C due to the formation of a protective layer of silica. Its thermal shock properties have been investigated extensively by Joseph Lucas Ltd., and by Newcastle University and it has been found that a crucible made from silicon nitride shows no ill effect when molten metal and water are alternately poured onto it (Arrol, 1973). Further, the crucible displayed no signs of chemical reaction when the molten metal had been heated in it for periods of up to 30 minutes. The modulus of rupture of silicon nitride is of the order of 60,000 psi.

Although silicon nitride does possess extremely attractive refractory properties there are three limitations that must be improved before it can fulfil its true potential. These limitations are:

i) the decrease in oxidation resistance above 1500°C

ii) the decrease in strength at high temperatures due to the softening of the glassy phases present

iii) fabrication difficulties, particularly inconsistency from batch to batch.

One way to overcome the second difficulty is to develop a ceramic with a more refractory bonding glass phase. This has been done by producing a new range of special ceramics from silicon nitride and another important refractory, alumina. As will be discussed in depth in Chapter 2, these two compounds will form a solid solution

in each other.   This new range of special ceramics, the sialons
(see for example Jack, 1976), have been shown to have improved
oxidation resistance; bend strengths of better than 100,000 psi
which do not decrease markedly with increasing temperature have
been reported by Arrol (1973).   The difficulties associated with
fabrication have not been removed yet; however, they are certainly
no worse in the sialons than they are in the original silicon nitride.

An added advantage of the sialons over silicon nitride is the
range of composition which is available giving a versatility that
could not otherwise be achieved.   Sialons have the composition

$$Si_{6-z}Al_zO_zN_{8-z}$$
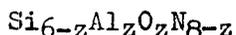
where z may vary from 0 to about 4.2.   The range of properties
available can be further extended by adding dopants to the lattice;
in particular magnesium, sodium, lithium and yttrium sialons have
been fabricated.   These dopants, together with the possibility of
altering manufacturing conditions result in a range of ceramic
materials with immense potential in high temperature industrial
applications.

1-2 Scope of the Present Work

This thesis is concerned with the electrical properties of one
group of the sialons, namely the lithium sialons.   There has been
very little previous work carried out on this topic, or indeed on
the electrical properties of any sialons. Jama, in a Ph.D. thesis
(Jama, 1975) made a preliminary study of the decay of the d.c.
conductivity of a lithium sialon and Sharif at Durham University is
carrying out a study of the electrical properties of undoped sialons,
(Thorp and Sharif, 1976). He has measured the a.c. and d.c. electrical
conductivities of two pure sialons (z=3.2 and z=4.0) and also silicon
nitride between 400° and 1,000°C.   The results of this work are re-
ported in Chapter 6 as a comparison to the behaviour of lithium doped

sialons.   Sharif also investigated the Hall effect and made measurements of the thermoelectric power in the two undoped samples.

Before the present work had progressed very far it was realised that sialons, and in particular lithium sialons are not well behaved as regards correlating their electrical behaviour with starting composition.   The reason for this may be intrinsic or it may be that differences in the ratio of the various phases present or even differences in the sizes of the crystallites in the material are having a major effect on the electrical behaviour.   It was therefore decided to approach the investigation of the electrical properties from two angles.   Firstly, the behaviour of the lithium sialons as insulators was studied;   this was intended purely to document the insulation properties of the lithium sialons and to give a picture of their value if used as insulating materials.   This study was confined to the temperature range 20° to 870°C and the results are presented in Chapter 4.

In the second part of the work an attempt was made to deduce the conductivity mechanism operating in the lithium sialons.   This was undertaken using a bridge method to measure the conductance and parallel capacitance of the sample, hence giving data that could be correlated with the different conduction mechanism models that might be applicable.   The results of the investigation, together with the relevant theory are discussed in Chapter 5.   Chapter 6 considers the effect of adding dopants to the lattice on the electrical behaviour by comparing the results obtained on lithium sialons with data on pure and yttrium doped sialons.

CHAPTER 2

PRODUCTION, COMPOSITION AND ANALYSIS OF SIALONS

2-1 Fabrication of Nitrogen Ceramics

Perhaps the major reason why silicon nitride has not made the inroads into the ceramics industry at the rate that would appear probable from looking at its excellent refractory properties, is the difficulty associated with its fabrication.   These properties, as outlined in Chapter 1 are far more likely to occur in a predominantly co-valently bonded solid, such as silicon nitride.   However, the self-diffusivity of such a co-valently bonded solid is extremely small with the result that it cannot be sintered to maximum density by firing alone.   There are two methods of producing solid silicon nitride that are now used, namely reaction bonding and hot-pressing.

Reaction bonding involves nitriding a silicon compact which has been made in the form of the required finished product.   This nitriding is carried out in molecular nitrogen at about 1400°C which yields a mixture of the two forms of silicon nitride, α and β.   The advantage of reaction bonding is that intricate shapes can be manufactured since there is very little dimensional change to the compact during nitriding;   it is also the cheaper method.   However, the theoretical density cannot be achieved by this technique and porosities of 25% are typical.   The low density results in some disadvantages, chiefly that a lower than maximum strength of the product is obtained and also that the oxidation resistance and resistance to corrosive environments is reduced because of the increased surface area.

The second method of forming silicon nitride is hot-pressing.   In this case, powdered silicon is first nitrided so as to give α-silicon nitride powder.   This is then hot-pressed in air at between one and two tons psi in a graphite die at about 1700°C.   This yields a maximum density, β-silicon nitride product with higher strength and

greater chemical resistance associated with it as compared to the reaction bonded material. However, the process is limited to simple shapes and is costly. It is not possible to use normal machining processes such as milling and turning on hot-pressed materials and cutting and grinding can only be carried out with great difficulty, whereas reaction bonded products can be machined in the normal way.

The method of hot-pressing has been extended and used by the research workers at the Department of Metallurgy, Newcastle University to manufacture the sialons investigated in the present work (Jama, 1975). The starting materials, shown in Table 1 were mixed using wet milling or by dry mixing in bottles on a Pascal ball mill. The grinding medium used in the wet milling was either cyl-peb alorite (Al_2O_3) or tungsten carbide balls, but with the latter tungsten was always observed as an impurity in the product. After mixing, the milled slurry was dried and the dry powder was vibromixed for a short time. In both cases the mixture was then vacuum dried at 100°C over phosphorus pentoxide to absorb water. The dry and thoroughly mixed powder was finally made into a pellet to be hot-pressed. In order to hot-press these mixtures it was necessary to add 1 to 2 wt% MgO to the starting materials. The pellet was buried in boron nitride and put into a graphite die; the boron nitride minimised the reducing effects of the graphite. A pressure of about 1 ton psi (154 bars) was applied to the die which was then heated to a temperature of between 1550 and 1700°C, usually 1650°C. This temperature was maintained for half an hour after which the system was allowed to cool naturally. Due to the high volatility of most lithium compounds, weight losses occurred in the majority of the products containing them as one of the starting materials. For this reason it was necessary to analyse chemically all the sialon products investigated as will be described later in this chapter.

Improvements are continuously being made in hot-pressing and

TABLE 1

THE STARTING COMPOSITIONS AND RESULTANT PHASES OF THE SAMPLES

Sample	Starting Composition $LiAl_5O_8$	Si_3N_4	AlN	h.p. temp$^{\circ}$C	Phases
Li 7	19.4m/o			1650	96%β', 4%Eu'
Li 8	28.4m/o	62.3m/o	9.3m/o	1650	95%β'
Li 22	30m/o	60m/o		1650	98%β', 2%X
Li 14	40m/o			1850	98%β', tr15R
Li 26	46m/o	53m/o	1m/o		
Li 15	46.3m/o	46.3m/o	7.4m/o	1650	60%β', 25%15R, 10%Eu', 5%Spinel
Li 30	9.4m/o	85.3m/o	5.3m/o oAl_3O_3N	1700	90%β', 10%12H
Y 28	14.3m/o Y_2O_3, 28.6m/o oAlN, 57.1m/o $oSiO_2$			1650	98% glass, 2%X

reaction bonding techniques.   However, it seems unlikely that it

will ever be possible to produce silicon nitride without a surface

coating of silica.   Apart from being an impurity this has the added

disadvantage that when silicon nitride is used as a starting material

for making sialon compounds, the silica layer prevents the production

of a single phase, homogeneous end product.   The ceramic will contain

at least two phases and in the instance where a second phase is a low

melting point vitreous one, as often happens, the product will tend

to soften at elevated temperatures with a consequent decrease in the

high temperature creep strength.   Any second phase will almost certainly

possess a thermal expansion coefficient different from that of the first;

as the temperature is varied this will cause stresses within the material

which in turn increases the possibility of cracks developing.

2-2 Structural Aspects of Pure Sialons

In the same was as the silicates can be derived from silica, SiO_2,

a range of nitrogen ceramics can be developed from silicon nitride, Si_3N_4.

The basic building unit of the mineral silicates is the SiO_4 tetrahedron;

each of these tetrahedra has a formal charge of -4 electronic units.

The tetrahedra can be joined in a number of ways leading to the diverse

properties of the silicates.   Some examples of the different ways in

which the tetrahedra can be linked are shown in Fig. 2i.   An irregular

array gives an amorphous structure as in the silicate glasses.

In a similar way nitrogen can form a tetrahedral structure with

four nitrogen corners surrounding a central silicon atom.   For example,

β-silicon nitride is a covalent solid built up of SiN_4 tetrahedra

joined by sharing corners in a three dimensional network, Fig. 2ii.

It would appear that α-silicon nitride is similar but seems to be a

defect structure with one in every thirty nitrogen atoms replaced by

an oxygen atom.

Aluminium plays a very important role in the silicate structures

in that the aluminium atom can form a tetrahedron with four oxygen

atoms in the same way as does silicon. Furthermore, the AlO_4 tetrahedron is approximately the same size as the SiO_4 tetrahedron; however, it has an overall negative charge of five units as compared with the -4 units for SiO_4. Hence it is possible to substitute the AlO_4 tetrahedron into a silicate structure if valency or other charge compensation is made elsewhere in the matrix. Since nitrogen will form a tetrahedral structure with aluminium and silicon in a similar way to oxygen, it is possible to use a nitrogen based compound to achieve the required charge compensation. This can be done in silicon nitride if for every Si^{4+} replaced by an Al^{3+}, one O^{2-} is substituted for an N^{3-}. Also other metal ions, e.g. Li^+, Na^+, Mg^{2+}, Y^{3+} can be introduced in addition to Al^3 in order to effect charge compensation. Even without the extra degree of freedom afforded by the introduction of these other metal ions a vast range of materials, both glassy and crystalline should be possible using silicon-aluminium-oxygen-nitrogen tetrahedra in a way analogous to that found in the range of silicates built from silicon-aluminium-oxygen tetrahedra. The acronym 'sialon' is now given to all materials based upon the structural unit $(Si, Al) (O,N)_4$ or more generally $(Si,M) (O,N)_4$, where M is one or more of the charge compensation metals above.
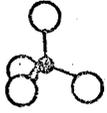
Early experiments to produce sialons involved hot-pressing silicon nitride, Si_3N_4 and alumina, Al_2O_3, together at high temperature (about 2,000°C). From X-ray powder photographs it was found that the structure of the resulting sialon remained essentially the same as that of hexagonal β - silicon nitride up to concentrations of Al_2O_3 of 70 wt%. Hence this crystalline phase was termed β'.

It is now clear that the composition of β' sialon is given by:

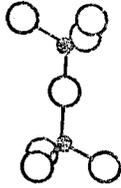$$Si_{6-z} Al_z O_z N_{8-z}$$
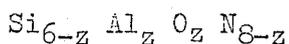
where z can vary from 0 to about 4.2. The derivation of this is explained by Jack (Jack, 1976). It will be noticed that this composition lies on the Si_6N_8-Al_3O_3N join. It was found that composition on the original Si_3N_4-Al_2O_3 join contained a relatively large amount of glassy phase as well as β', while those compositions with a metal to non-metal ratio: 3:4, i.e. that of the original Si_3N_4 showed

orthosilicates SiO_4^{4-} pyrosilicates $Si_2O_7^{6-}$ ring silicates $Si_3O_9^{6-}$
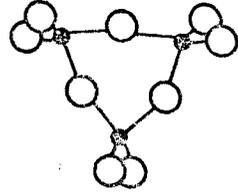
eg olivine   eg melilite   eg wollastonite

ring silicates $Si_6O_{18}^{12-}$ single chain silicates $(SiO_3)_n^{2n-}$
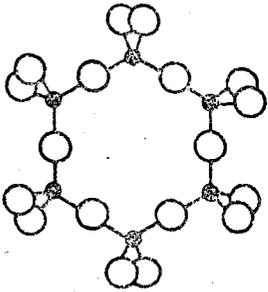
eg beryl   eg pyroxene

double chain silicates $(Si_4O_{11})_n^{6n-}$

eg amphibole

FIG. 2i   The Silicate structures (after Kingery)

⬤ = Silicon

◯ = Oxygen

FIG. 2ii   The crystal structure of
β - sialon nitride. (after Jack)

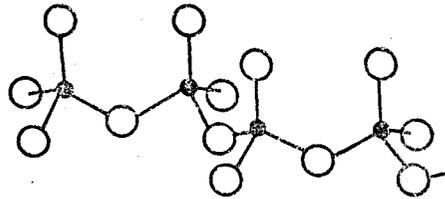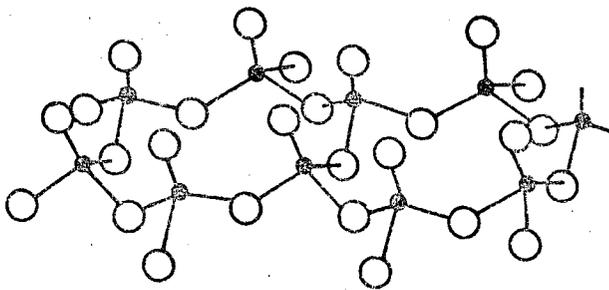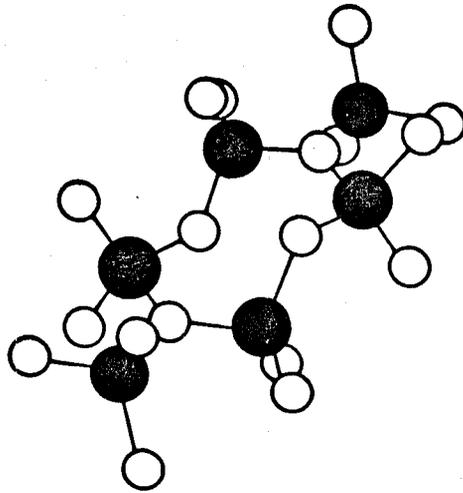minimum high temperature creep, indicating a lower glass content since a vitreous phase would increase high temperature creep. The range of homogeneity where $M:X \neq 3:4$ is quite small. It is now known that most, and certainly all the sialons studied in the present work comprise β' crystals within a glassy matrix. This can be seen from transmission electron micrographs, one of which is shown in Fig. 2iii. The presence of the β-silicon nitride crystal in this photograph indicates that the glassy phase contains nitrogen.

As mentioned before, every particle of Si_3N_4 powder is always coated with a very fine layer of silica. Attempts to remove this, e.g. by washing in caustic soda, reduce the quantity present but leave an indeterminable amount behind. For this reason the Newcastle research workers made the assumption that there was 4 wt% of silica in the starting material and compensated for this by adding 2AlN for each SiO_2. In this way the final compositions were kept as near to the $M:X = 3:4$ line as possible.

2-3 Extension to Lithium Sialons

The original approach towards making lithium sialons was to use a "pure sialon" mix and hot-press it with lithia, Li_2O, i.e. to go from some sialon composition on the $Si_3N_4 - Al_2O_3$ base line to the top corner of the phase diagram shown in Fig. 2iv. This proved undesirable since Li_2O volatilizes readily causing large weight losses and hence the exact composition of the end product was not easily predictable. However, various lithium aluminates can be used and most of the present work was concerned with samples which were made from $Si_3N_4 - LiAl_5O_8$ (lithium spinel) mixtures. The compositions of the samples examined are listed in Table 1.

For compositions with spinel concentrations of up to 50m/o $LiAl_5O_8$ (i.e. all those investigated in the present work) the crystalline constituent of the resultant lithium sialon was almost entirely β' phase with up to 5 wt% of X-phase. The latter, the so-called X-phase is now known to be a monoclinic phase and tends to be alumina rich.

FIG. 2iii   Transmission electron micrograph

of hot-pressed silicon nitride with amorphous

region "A" from which has grown a well-defined

hexagonal β-Si_3N_4 crystal, x20,000.

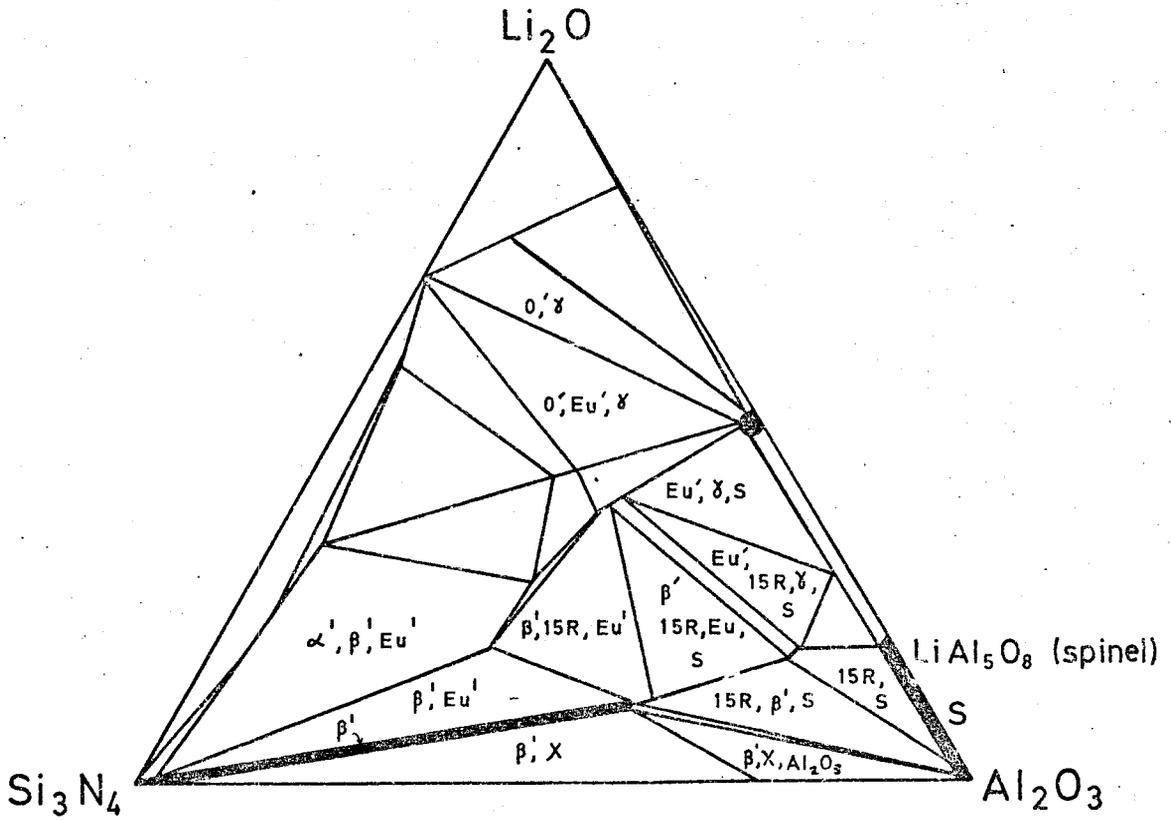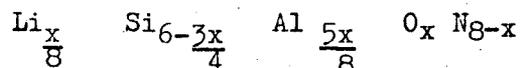(Reproduced by permission of Prof. Jack,
 University of Newcastle)

FIG. 2 iv   The Li_2O - Si_3N_4 - Al_2O_3 section of the
Li - Si - Al - O - N system at 1550°C. (after Jack)

The range of compositions of β' lithium sialons is given by

$$Li_{\frac{x}{8}} \quad Si_{6-\frac{3x}{4}} \quad Al_{\frac{5x}{8}} \quad O_x \, N_{8-x}$$

where x and 8-x are the numbers of oxygen and nitrogen atoms respectively in the unit cell.   Again the β' phase is restricted to compositions where M:X is 3:4, which is the case for all compositions in the Si_3N_4 - $LiAl_5O_8$ series.   Other phases that can occur with high lithium spinel concentrations are Eu' (based on β - eucryptite), O' (based on silicon oxynitride), and γ (based on tetragonal cristobalite).   The compositions of these phases are shown in the $Li_2O-Si_3N_4-Al_2O_3$ phase diagram which is drawn in Fig. 2iv.   As for pure sialons there is evidence to suggest that in β' lithium sialons a glassy phase is present.

2-4 Yttrium Sialons

In order to hot-press either silicon nitride or sialons a small amount, 1-2 wt%, of MgO is required in the starting mix as mentioned in section 2-1.   This is needed to form a glass which will soften at the hot-pressing temperature and so increase the flow between grains when pressure is applied.   As a result of this, the cooled sialon contains a magnesium-silicon oxynitride glassy phase at the grain boundaries which has a variable softening point often well below the hot-pressing temp-erature.   If yttria, Y_2O_3, is used as the additive in place of magnesia, a more refractory grain boundary phase is achieved.   In the Y_2O_3 - SiO_2 system the lowest liquid temperature is $1660^{\circ}C$.   The idea of using an yttrium additive has been extended to form yttrium sialons, and one of these, the composition of which is given in Table 1, has been studied in the present work for comparison with the lithium sialons.   It dif-fered from the lithium sialons in one important feature; it was pro-duced such that it comprised as much glass as possible.   Microscope analysis at Newcastle has shown that it was made up of about 98% glassy phase, the remainder being a crystalline β' sialon phase.

By comparing the properties of the yttrium sample with those of an

"ordinary", predominantly crystalline lithium sialon it was hoped to gain some information of the role of the glassy matrix in the electrical behaviour of lithium sialons. Unfortunately, it was not possible to obtain a lithium sialon glass.

2-5 Chemical Analysis of Samples

Weight losses of between 1 and 11% were recorded for lithium sialons in the composition range 20-33 m/o $LiAl_5O_8$, 80-67 m/o Si_3N_4 (Jama, 1975). To investigate the composition of the final sialon produced, samples were analysed chemically by the Department of Chemistry at Durham University. In outline the method of analysis adopted was as follows.

Samples were crushed and put through a 53 micron sieve. It was then necessary to get the powder into solution; this proved to be extremely difficult. The first solvent tried was a mixture of HF and HClO in which the powder was fused under a I.R. lamp. However, this usually left an insoluble white residue. The second method of dissolving the powdered sample was to fuse it with Na_2CO_3 and then acidify it with HCl. This gave a clear solution. The solution was then analysed using atomic absorption spectroscopy for lithium, silicon and aluminium. The errors associated with these analyses occurred when trying to get the powders into solution; although the solutions appeared to be clear when sodium carbonate fusion was used the difficulty in obtaining this solution implies that there it is not a perfect one. Unfortunately, it is very difficult to judge how good a solution has been obtained and therefore the overall accuracy of the chemical analysis is probably no better than $\pm$ 0.1% of weight of element found. The error on the spectroscopy is negligible, in the region of .01% of the weight found of the element. The analyses obtained are shown in Table 2.

One of the samples was also sent to the Analytical Services Laboratory, Imperial College of Science and Technology, where the lithium content was determined by a similar atomic absorption method. The comparison of the analyses on the sample, which had the starting composition

TABLE 2

CHEMICAL ANALYSIS DATA FOR LITHIUM SILLOYS

Sample No.	Lithium		Aluminium		Silicon	
	Starting Composition	Final Product	Starting Composition	Final Product	Starting Composition	Final Product
Li 30	0.43	0.28	11.15	10.57	47.02	41.86
Li 2	0.46	0.33	8.82	7.6	49.41	43.99
Li 8	1.17	0.99	24.02	22.56	31.59	27.68
Li 15	1.40	0.97	27.89	26.32	16.84	15.84
Li 14	1.46	0.72	28.13	18.57	26.25	33.24
Li 26	1.62	0.79	31.44	20.74	22.39	28.27

(All figures refer to weight per centages).

$30m/o$ $LiAl_5O_8$, $68m/o$ Si_3N_4, $2m/o$ AlN is as follows:-

Starting composition	Durham University	Imperial College
1.16 wt%	.65 wt%	.65 wt%

which shows that the two laboratories were in excellent agreement.

CHAPTER 3

EXPERIMENTAL TECHNIQUES

The aim of the present work was to measure the electrical conduction properties of different lithium sialons and one yttrium sialon as functions of frequency and temperature. This was done in two different ways. Firstly the insulation behaviour, i.e. the way in which these materials would behave in industrial applications was investigated. Secondly, the conductivity and dielectric behaviour of the sialons were studied to investigate the conduction mechanism operating in the samples by comparing their measured electrical behaviour both with theory and with experimental results for other similar ceramics, particularly undoped sialons. Further, it was of interest to compare the behaviour of lithium sialons with that of the yttrium sialon sample which was known to be 98% glass.

The lithium sialons studied ranged in lithium content from 10m/o $LiAl_5O_8$ to 46m/o $LiAl_5O_8$. The composition of the yttrium sialon as well as the other samples studied is shown in Table 1.

3-1 Sample Preparation

The sialons were received from Newcastle University as irregular shaped blocks of varying sizes. It was decided to make measurements on samples in the form of bars of the order of 1.5 x 0.3 x 0.4cm in size in order to reflect the bulk properties of the material. However in some cases it was necessary to use smaller samples when these were all that were available or if a sample showed an internal fault, such as a crack, when it was cut. The possibility of such cracks in the samples used cannot be ruled out but care was taken to use samples where this seemed to be unlikely. Work on samples other than lithium or yttrium doped sialons has been carried out by others (Thorp and Sharif, 1976).

The hardness of all the sialons required that they be cut on a diamond cutting wheel; this proved quite practicable although it did

result in considerable wear of the wheel.

Contacts for the measurement of electrical conduction at high temperature were made using platinum paste supplied by Johnson Matthey Metals Ltd. A sample was washed in acetone and then the two end surfaces were smeared with a thin layer of the platinum paste. This was dried with a hot air blower. The thin layer ensured good electrical contact over the entire end surfaces. Platinum paste was then packed over these two layers and a small piece of platinum wire (about 1cm in length) was pushed into the paste at each end of the sample. The sample plus contacts was then baked at 600°C for one hour to harden the platinum paste. A sample with contacts is shown in Fig. 3i.

A small amount of work was carried out at room temperature using gold contacts for reasons to be discussed in section 3-3-2. To make these contacts a sample was washed in acetone as before and then a thin layer of gold was evaporated onto the end surfaces using an Edward's High Vacuum Coating Unit. A similar gold layer was also evaporated onto the detachable brass plates of the jig, shown in Fig. 3ii, which was used to hold the sample.

3-2 Sample Mountings

In the high temperature studies one of two similar Kanthal wire wound furnaces of resistance 76Ω and 34Ω was used. The furnace tube bore was 3.7cm in both cases. The sample was introduced into the hottest part of the furance as shown by the plateau of the temperature profile of the furnace. One of the profiles is shown in Fig. 3iii. The upper limit of temperature was set by the limitations of the furnaces and was found to be about 870°C. All the experiments were conducted in air.

The sample mounting used to support the sample in the furnace tube comprised three similar pyrophyllite discs 3.7cm in diameter and 4mm thick. Each of these had three holes drilled in it in a

PLATINUM PASTE

PLATINUM WIRE

·3cm

·4cm

1·5cm.
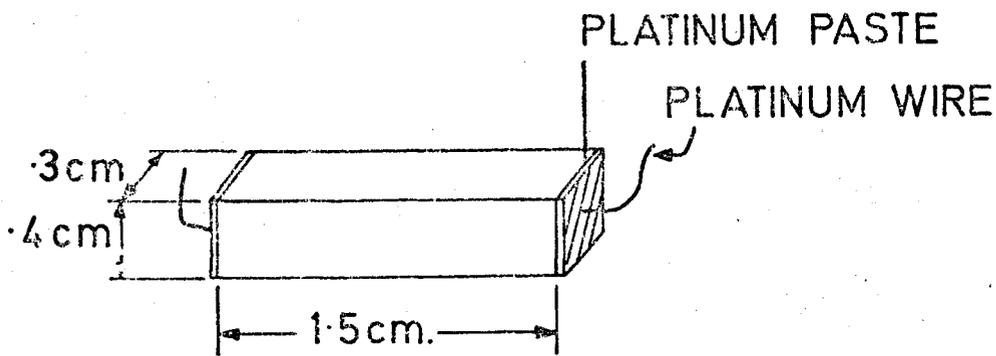
FIG. 3i Details of specimen contacts showing typical size of specimen.
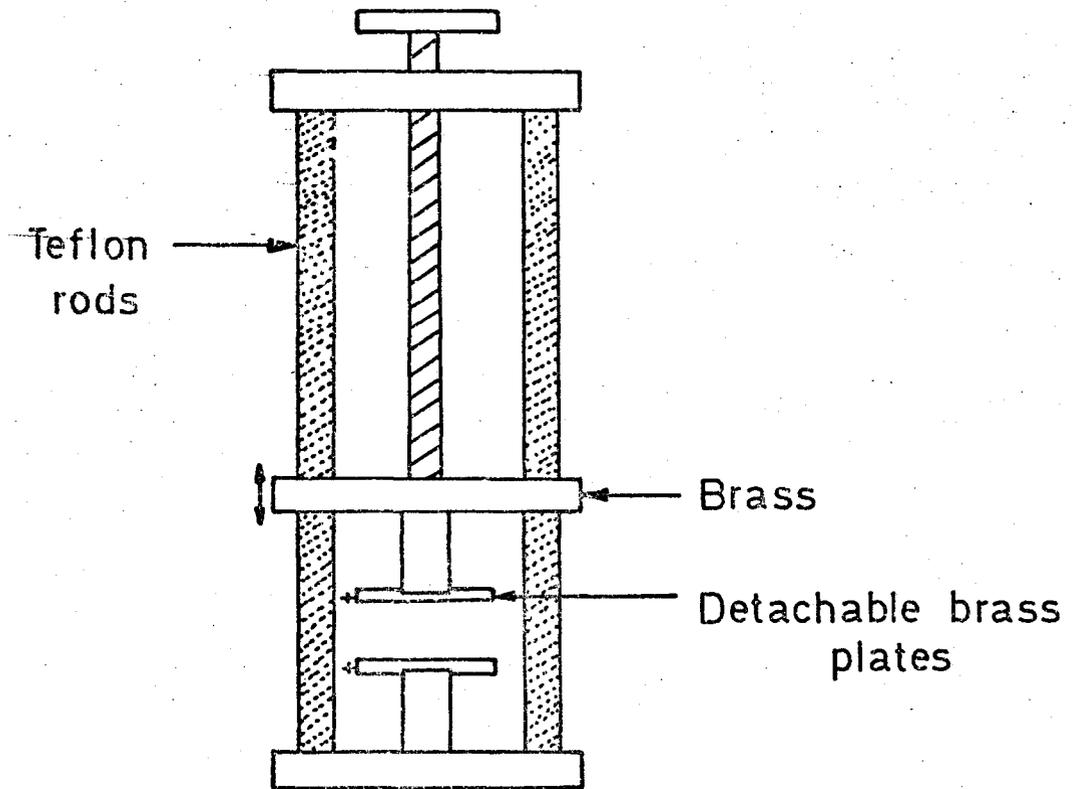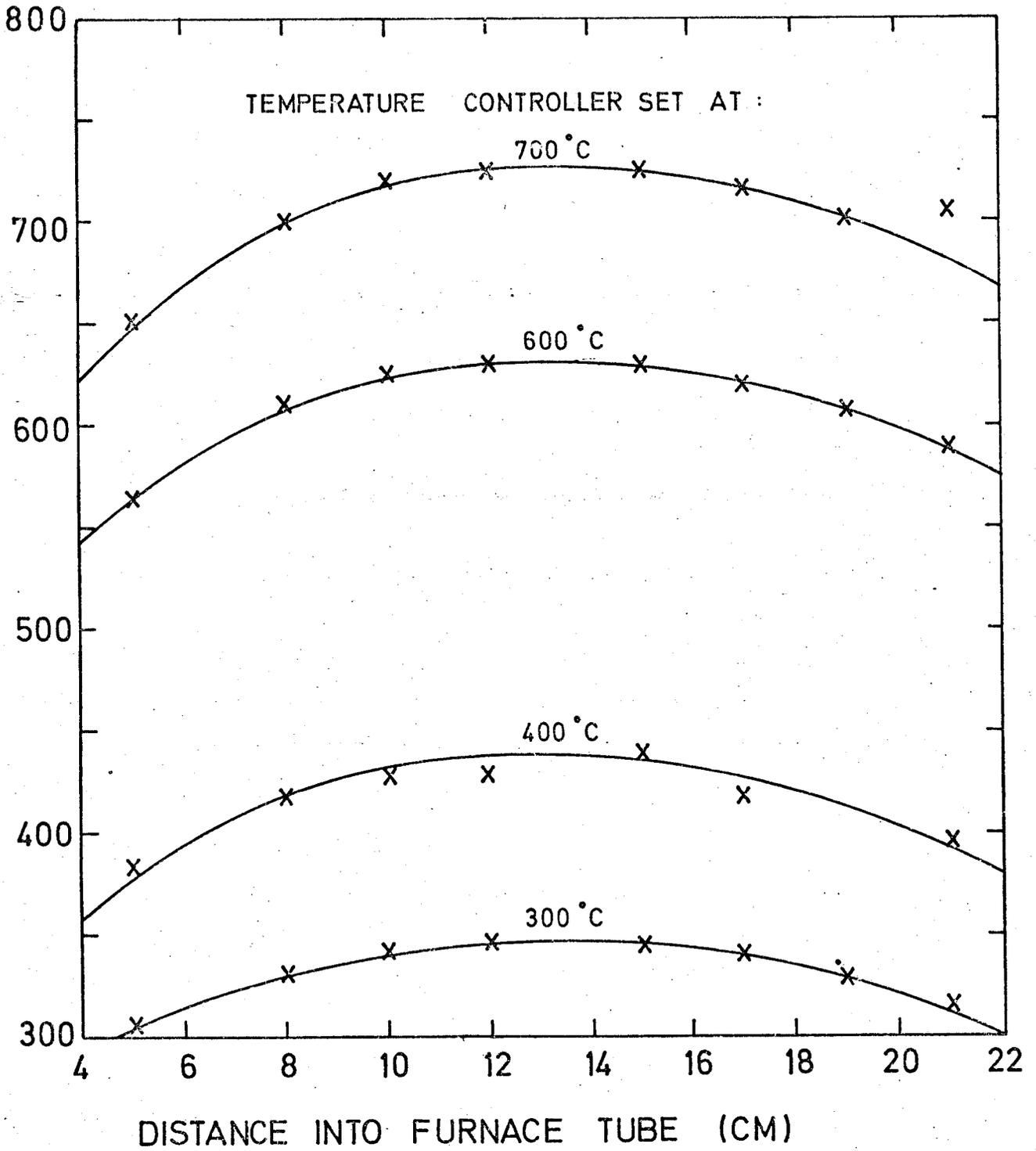
Teflon rods

Brass

Detachable brass plates

FIG.3ii Jig used at room temperature for bridge measurements on samples with gold contacts.

FIG.3iii. Temperature profile of Furnace 1.

line. Through these holes three silica tubes were supported. The centre tube was four bore and carried the two platinum/13% platinum rhodium thermocouples. One of these was used in conjunction with an Ether Temperature Controller to maintain the furnace at the temperature set to within $10^{\circ}C$. The other thermocouple was connected to a Pye Portable Potentiometer which measured the temperature to within $5^{\circ}C$. Two platinum lead wires were carried down the outer silica tubes, which kept them as physically far apart as possible, and were spot-welded to the platinum wires of the sample contacts. These two silica tubes protruded $\frac{1}{4}$ inch beyond the centre, thermocouple tube. In this way the sample was kept not only at the same height in the furnace as the thermocouples but no more than 3/8 inch from them.

3-3 Electrical Measurements

3-3-1 Insulation Behaviour

The insulation conductivity in both the d.c. and a.c. cases was investigated by applying a voltage across the sample and measuring, directly or indirectly, the current that flowed as a result.

It was known from an earlier study (Jama, 1975) that lithium sialons are unstable under d.c. conditions. The apparent solid state electrolysis that occurred was investigated in the present work using a simple circuit which comprised a Farnell d.c. Power Supply in series with a sample and a moving coil galvonometer of maximum sensitivity .0046 $\mu A/mm$. Thirty volts was applied across the sample for periods of up to 500 hours. The sample was maintained at $600^{\circ}C$ to increase the current flow and so augment the degradation effects. The value of the current flowing was monitored at regular intervals throughout the experiment.

The a.c. insulation conductivity of the lithium sialons was investigated using the circuit shown in Fig. 3iv in which a steady a.c. voltage was supplied across a Jay-Jay decade resistance box and a sample in series with it. Two similar digital multimeters monitored
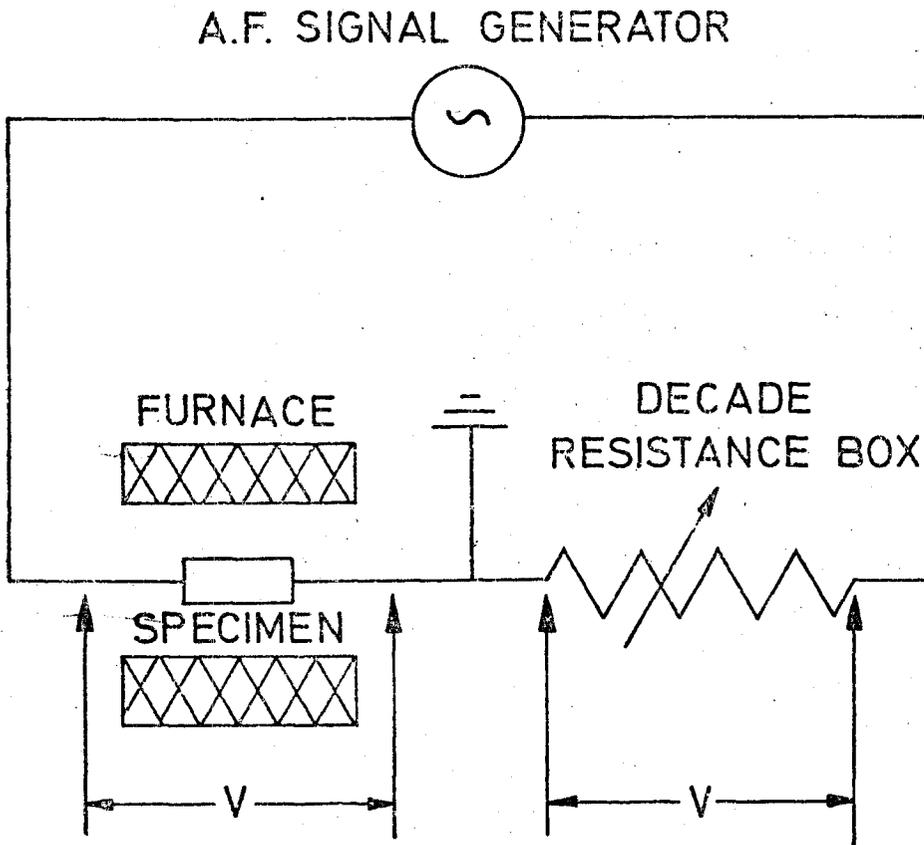
FIG. 3iv Technique used for measuring a.c. insulation resistance as a function of temperature.

the potential drop across the resistance box and the sample respectively; the value of the former was adjusted until the two potential drops were the same. Hence if R is the resistance of the sample and R_s is that of the resistance box then when both potential drops are the same

$$R = R_s$$

since the same current is flowing through each. The a.c. insulation conductivity, $\sigma_{ac}(ins)$ is then given by

$$\sigma_{ac}(ins) = \frac{1}{R_s} \times \frac{L}{A}$$

where L is the length of the sample between the electrodes and A is the electrode area.

Using this technique $\sigma_{ac}(ins)$ could be determined within the frequency range 20Hz to 25kHz and from room temperature to 870°C.

3-3-2 Conduction Mechanism Measurements

In order to investigate the conduction mechanism operating in a material it is necessary to measure both the a.c. and d.c. conductivities in ways considerably different from those used in the preceding section. In the d.c. case it was required to minimise the degradation effects and for the a.c. measurements to remove the capacitive component from the conductivity.

The d.c. conductivity of a range of samples was investigated as a function of temperature using the circuit shown in Fig. 3v. The applied potential was kept small enough for no degradation effects on the sample to be detectable, (usually this potential was less than 5 volts). Also the voltage was applied only when a reading was to be taken and not maintained between readings. The voltage drop across the standard resistance (typically 10^5 ohm) was measured using an f.e.t. d.c. amplifier, partly to amplify the signal and so permit lower voltages to be applied overall but also so as to provide the voltmeter with an effective input impedence of 10^{13} ohm. This was orders of magnitude higher than that of either the sample or the standard resistance. In this way a true reading was obtained which was not affected by the leakage of
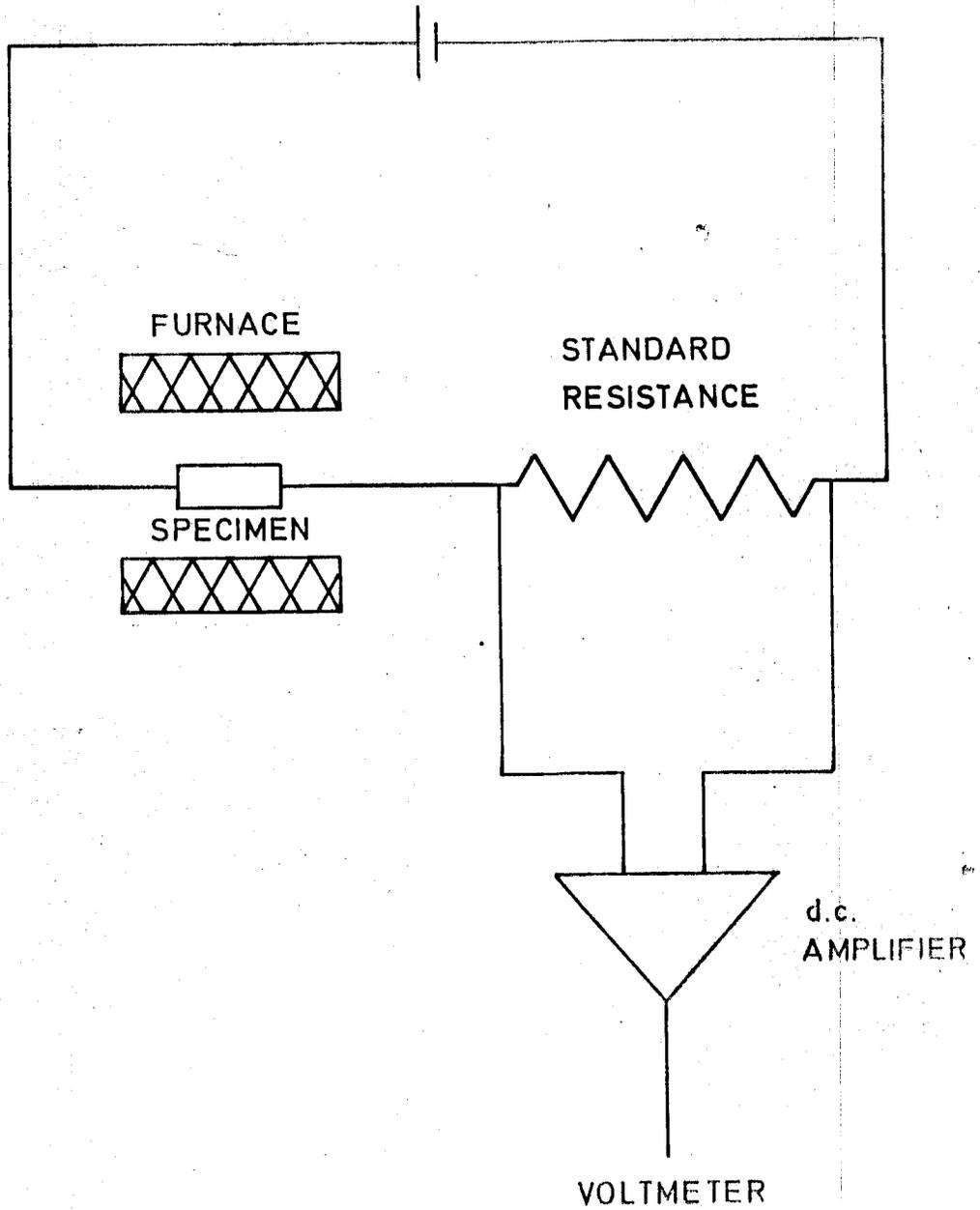
FIG. 3v   Circuit used to measure d.c. conduction at high temperature.

current through the voltmeter. The value of the resistance of the sample R, was computed as follows:-

$$V = i (R + R_s)$$

$$V' = V_s g$$

$$V_s = i R_s$$

$$\therefore \frac{V}{R + R_s} = \frac{V'}{R_s g}$$

$$\therefore R = \frac{R_s (Vg - V')}{V'}$$

where V is the applied voltage

R_s is the value of the standard resistor

i is the current

V' is the voltage read from the voltmeter

g is the gain of the amplifier

V_s is the voltage actually dropped across the

standard resistor

From the value of R, the d.c. conductivity σ_{dc} is given by

$$\sigma_{dc} = \frac{1}{R} \times \frac{L}{A}$$

The sizes of the samples were measured, using a micrometer screw gauge, to an accuracy of .001cm. The gains of the d.c. amplifier were measured at the different levels used and found to be 11.2 (nominal 10), 50.2 (nominal 50) and 101.2 (nominal 100). The lower limit of temperature for d.c. measurements of conductivity was 150°C - 250°C, depending on the sample; this limit was determined by the signal to noise ratio of the d.c. amplifier since the d.c. conductivity decreases with decreasing temperature.

In order to investigate the conduction mechanism in the lithium sialons it was necessary to separate the capacitive component from the a.c. conductivity. To do this a Wayne Kerr Parallel Capacitance Bridge was used; this provided two readings, the conductance G, and the parallel capacitance C of the sample. From these two readings the a.c. conductivity σ_{ac}, the dielectric constant ϵ', and the dielectric loss $\tan\delta$,

could be computed using the following equations

$$\sigma_{ac} = G \times \frac{L}{A} \qquad\qquad (3\text{-}1)$$

$$\varepsilon' = C \times \frac{L}{A} \qquad\qquad (3\text{-}2)$$

$$\tan\delta = \frac{G}{\omega C} \qquad\qquad (3\text{-}3)$$

The internal frequency of the bridge was 1.592kHz ($\omega = 10^4$) but by using an external power supply a maximum range of 500Hz to 3kHz could be achieved. Useful measurements could be made at temperatures down to 200°C at which temperature the conductance and capacitance of the sample mounting was no longer negligible compared to those of the sample.

Measurements made at room temperature using the bridge, employed the jig shown in Fig. 3ii. Using this jig it was possible to measure, and hence allow for, stray conductances and capacitances, which as mentioned above are no longer negligible at room temperature. To do this the conductance and capacitance of a sample were measured in the normal way; measurements were then repeated with the sample removed and the distance between the plates of the jig kept the same.

The correction terms were derived as follows:-

let G', C' be the conductance, capacitance of the sample+jig+stray
i.e. the normal bridge reading

" G_j, C_j " " of the jig

" G , C " " of the sample

" G_0, C_0 " " of the sample+stray i.e. the bridge reading with no sample

" C_a be the capacitance of the volume of air between the plates

" C_{as} " " same volume of air as that of the sample

Then the conductance of the sample is given by

$$G = G' - G_0$$

In the case of the capacitance

$$C' = C_s + C_j + C_a$$

$$C_o = \quad C_j + C_a + C_{as}$$

now $C_{as} = \dfrac{\varepsilon A}{L} = \dfrac{\varepsilon_o \, \varepsilon'_{air} \, A}{L}$ where A,L are the dimensions of the sample

$$\therefore C = C' - C_o + C_{as}$$

However C_{as} was found to be negligible as were end corrections and so both were ignored.

The room temperature values of the dielectric constant, loss tangent and the a.c. conductivity were computed as for the high temperature measurement from equations 3-1, 2 and 3 but using the corrected values for C and G. It was not possible to use this sort of correction on high temperature measurements as there was no way of ensuring that the distance between the platinum paste contacts with no sample between them remained the same as that with the sample in position.

The behaviour of the three parameters σ_{ac}, ε', and $\tan\delta$ together reflect the performance of the sialons as workable materials in the electrical sense. In theory it should be possible to compute from these three parameters the electrical insulation conductivity but due to the complex structure of these multiphase composite materials they behave as though $\sigma_{ac}(ins)$ and σ_{ac} were almost unrelated properties and hence it has been necessary to treat them separately.

3-4 X-Ray Methods

X-Ray methods were employed to investigate the effect on the crystal structure of the sialons as a result of the degradation caused by the application of a d.c. voltage. A Debye-Scherrer powder camera with a diameter of $4\frac{1}{2}$ inches was used in a beam of Cu K_α radiation produced through a Nickel filter. Samples were ground through a 53 micron sieve and then packed into capillary tubes. X-ray powder photographs were taken before electrolysis and pictures were taken from each end and the middle of the sample after current had been passed through it. A similar photograph was taken of a small amount of platinum paste on a

glass fibre so as it could be seen if any paste had diffused into the

sample. All of these photographs were kindly analysed by the Crystal-

lography Laboratory in the Department of Metallurgy at the University of

Newcastle; they are included in Appendix I.

3-5 Optical Absorption

In an attempt to estimate the band gap from optical absorption

measurements, samples were examined optically from 200 to 700 milli-

microns and from 2 to 40 microns. Following standard practice the

samples were crushed and made up into potassium bromide discs. No in-

formation could be gained as to the absolute value of the transmittance of

sialons using this technique since the amount of sample in the disc was

undetermined but the shape of each of the spectra was obtained. Some

spectra are shown in Appendix 2.

CHAPTER 4

RESULTS 1 - INSULATION BEHAVIOUR

The electrical conduction properties of a range of lithium sialons have been investigated using the techniques described in the previous chapter. In this chapter the results of the studies of the insulation behaviour of the lithium sialons are presented and discussed. These preliminary measurements were useful in establishing the general pattern of the conductivity behaviour. An attempt has been made to determine in which of the constituents of the material the conduction is taking place.

The insulation resistance refers to that resistance which a material would exhibit if it formed a connecting path between two area of differing electrical potential e.g. in an application as an insulator. Here the reciprocal of it is discussed in order to make comparisons with other sections easier. Hence in d.c. terms one is concerned with the insulation conductivity and in the a.c. case with the total admittance, here referred to as the a.c. insulation conductivity.

4-1 D.C. Insulation Behaviour

Firstly consider the d.c. properties of sialons under insulation conditions. It had been observed in earlier work carried out at Durham that the passage of a d.c. current resulted in a decrease in the d.c. conductivity. To investigate this an electrical potential, usually 30 volts was applied across the sample. This proved adequate to show quite a marked effect over a short period of time: merely heating up the sample while the potential was applied resulted in a cooling curve obtained as the sample cooled, (still with the potential applied), which was distinctly different from that shown by the sample as it was heated. This phenomenum is shown in Fig. 4i(a) by sample Li 15 (46m/o lithium spinel) and also by a sodium sialon, both of which are compared with a pure sialon in which the heating and cooling conductivities are the same. All the lithium sialons investigated showed the same behaviour. These
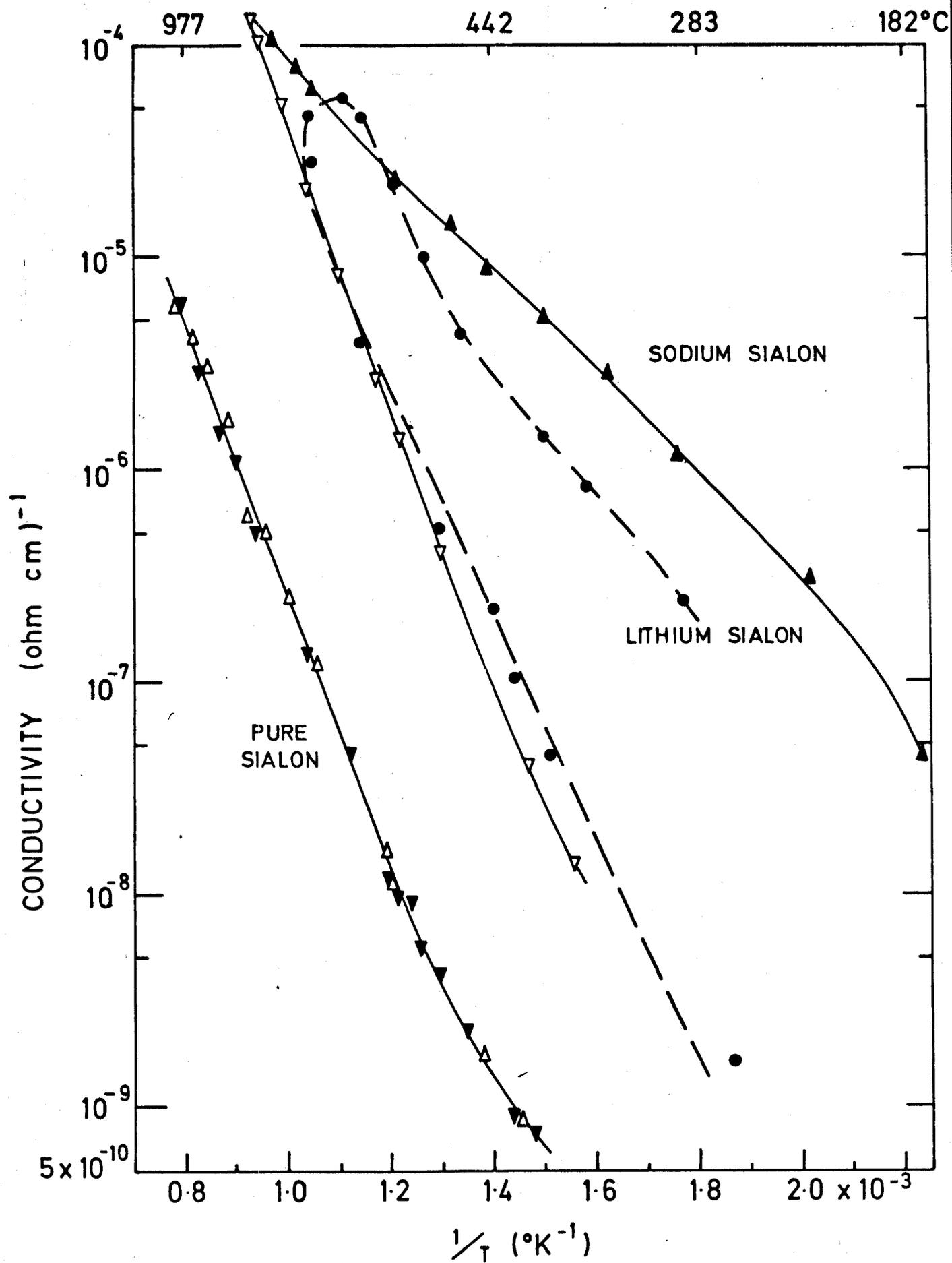
FIG. 4 i. The d.c. conductivity as a function of temperature in an undoped and a sodium doped and a lithium doped sialon.
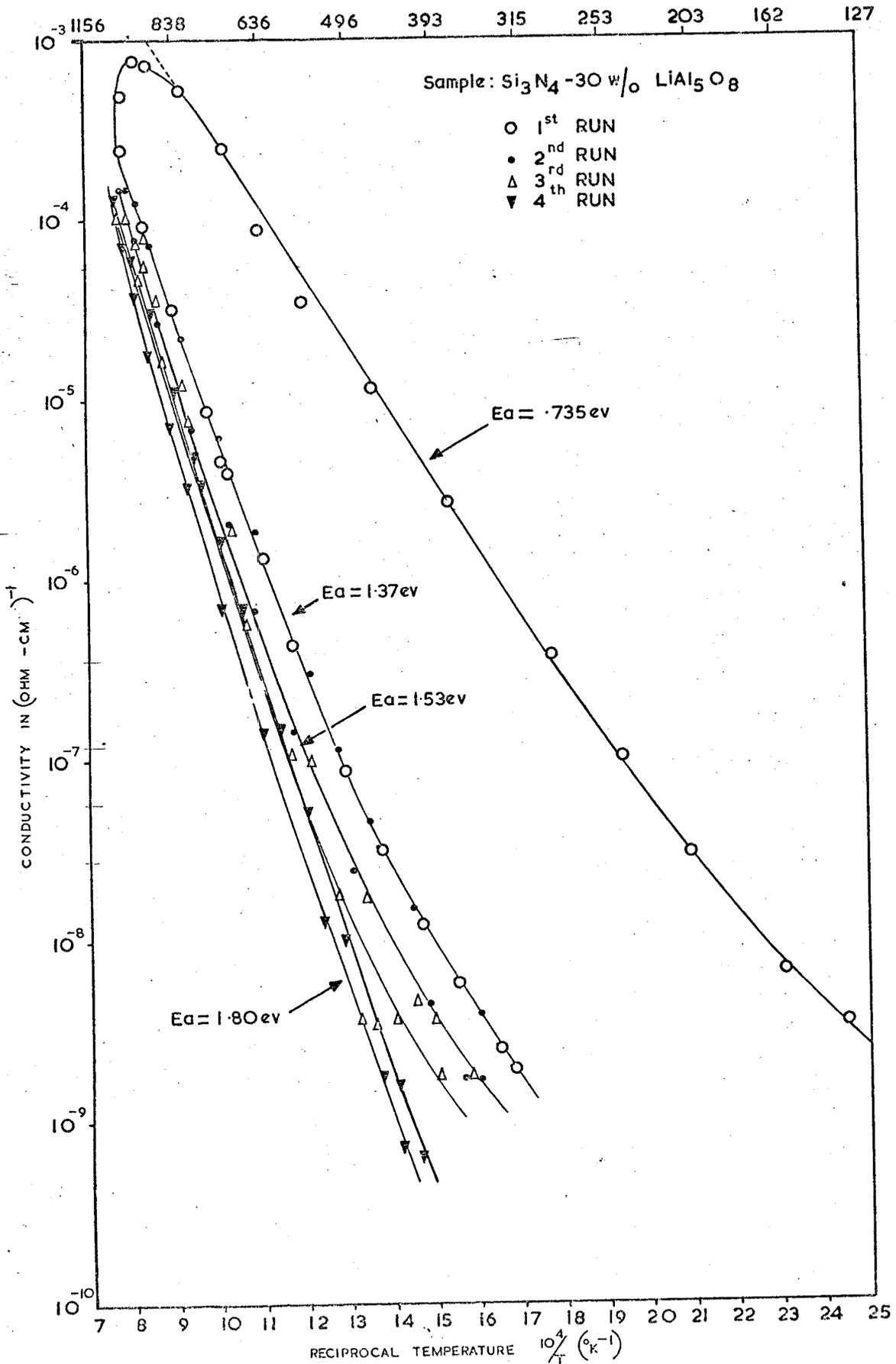
Fig 4i(b) D.C. Conductivities & Ageing Effects in Lithium Sialon.

observations confirm the earlier findings of Buckley and Sharif (unpublished) who made d.c. conductivity measurements on a 30w/o lithium spinel sialon about two years ago.   Their results are reproduced in Fig. 4i(b) and show an increase in the slopes of the conductivity curves implying a corresponding increase in the d.c. activation energy as temperature cycling proceeds.

A further study of this behaviour was made by investigating the conductivity of a lithium sialon at a fixed temperature as a function of time.   The results of this experiment are shown in Fig. 4ii.

The behaviour shown in Fig. 4ii could be attributable to some form of solid state electrolysis or diffusion taking place due to the lithium content.   An alternative possibility, that of polarization being the cause seemed to be unlikely due to the length of time for which the decay of the conductivity continued.   Furthermore, as discussed in Chapter 2, the crystallographic structure of pure and lithium sialons is very similar and so if the degradation were caused by polarization there seems no reason why the effect would be seen only in lithium and sodium sialons.   The theory that electrolysis or diffusion is the cause of the degradation was supported by the fact that a magnesium sialon showed only very slight differences in heating and cooling conductivities which is consistent with the relatively highly mobile alkali ions (i.e. Na^+ and Li^+) being responsible for the electrolysis in the lithium and sodium sialons.

If electrolysis were taking place it was thought possible that some crystallographic change in the sample might occur since a sample nominally containing 46.3m/o lithium spinel had shown that the conductivity decay was irreversible.   After this sample had been heated and then allowed to cool with a d.c. potential applied, the polarity of this potential was reversed;   on subsequent temperature cycling the conductivity continued to decay as though no polarity change had been made.   It was noticed that after a decrease in the d.c. conductivity had occurred the
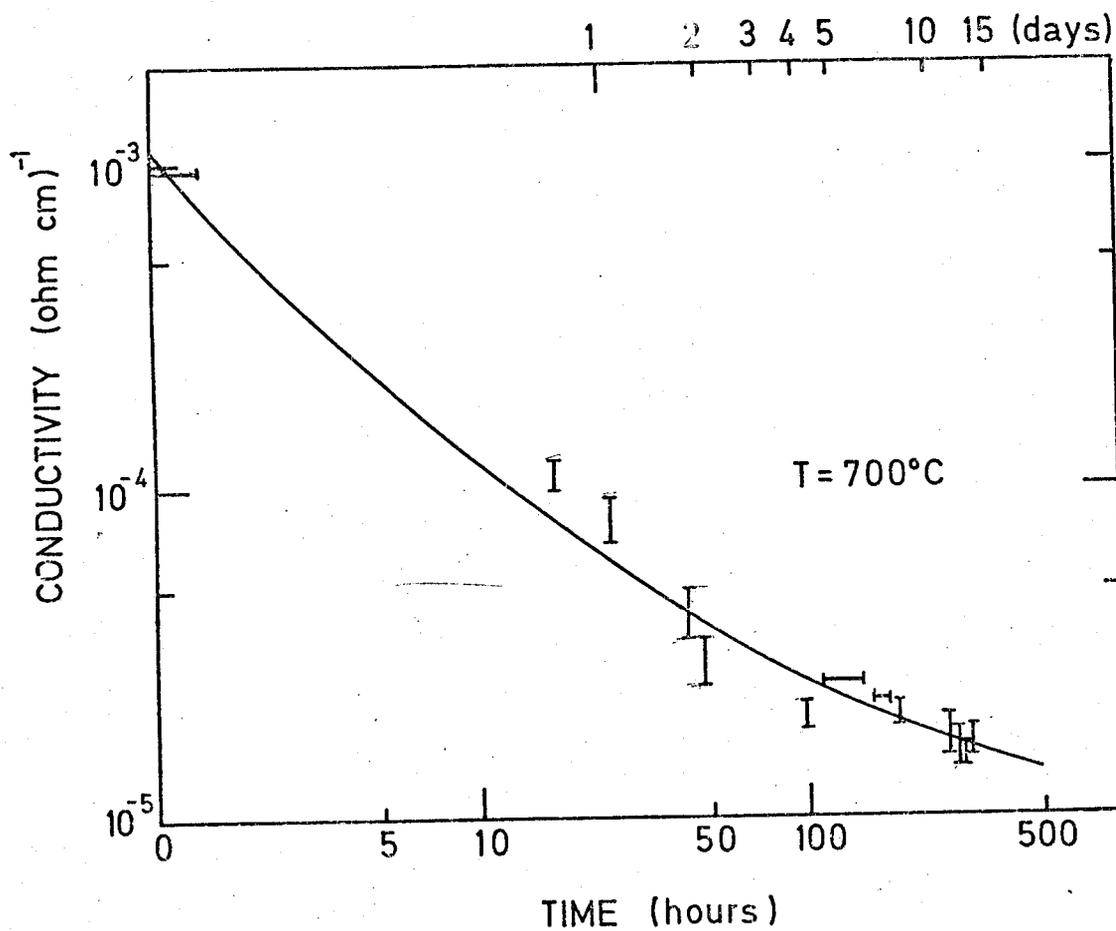
FIG. 4ii   Decay   of   the   d.c.   insulation   conductivity
with   time   in   30 m/o   Li   sialon.

sample had discoloured and showed a darkened area.   This discoloration always occurred but was not always in the same position;   often it was near to the positive electrode but sometimes developed nearer the centre of the sample.

X-ray powder analysis was used to investigate any structural change in the sample but the result was completely negative.   No evidence of any change was found.   There are several possible explanations for this:-

i) the limited period of treatment at 700°C did not cause a great enough effect to be seen on the X-ray powder photographs

ii) it was a surface effect rather than a crystallographic one

iii) polarization was responsible as discussed above

iv) the electrolysis was taking place in the glassy constituents of the sample which are invisible to the X-ray beam.

If case i) is correct, structural changes involving a compound with a small overall cross-section to X-rays is indicated.   Such a compound would most likely be a lithium one, such as lithia.   This explanation would account for the pure sialons not exhibiting degradation.

There is some evidence that most of the conduction, even in the d.c. case occurs along the surface of the sample.   If this is so then possibly the effect of being heated or passing a current is altering the surface by, for example, removing water vapour or other surface con-taminants.   However, if this were the cause of the degradation one would expect a similar decay in the a.c. conductivity and as this is not ob-served this explanation seems to be unlikely.

The most probable explanation seems to be that outlined in case iv) since, as will be shown later, there is strong evidence to suggest that the glassy phase is the major conducting medium.   However, there seems to be no way of proving this conclusively except by considerably more work on the glassy compounds present.   It is noteworthy that the colour differences mentioned above were very similar to those found between sialons of similar composition but of differing porosity.

4-2 A.C. Insulation Behaviour

The a.c. electrical insulation conductivity of sialons shows a very distinctive response to temperature. Over the temperature range investigated, 20° to $800^{\circ}C$, two conductivity regimes exist.

A typical set of results is shown in Fig. 4iii which refers to sample Li 26. It is useful in describing the a.c. insulation conductivity to separate the temperature axis into two regions. Region 1 extends from room temperature to some temperature, T_1 which depends far more strongly on the frequency of the applied potential than on the sample composition. In region 1 the a.c. insulation conductivity, $\sigma_{ac}(ins)$ is independent of temperature. There is then a transitional zone until at some temperature, T_2, $\sigma_{ac}(ins)$ becomes frequency independent and temperature dependent in region 2.

In region 1 the behaviour of $\sigma_{ac}(ins)$ can be described by

$$\sigma_{ac}(ins) = K_{\nu} \text{ where K is a constant at a given frequency, } \nu$$

and can best be examined by plotting $\sigma_{ac}(ins)$ at room temperature against frequency. This is done in Fig. 4iv. In this graph there would appear to be a slight increase in the conductivity with increasing nominal lithium content. Further work has indicated that the lithium sialon series is not so well behaved and only gross differences have any real effect, i.e. 46m/o Li spinel usually has a higher conductivity than does 10m/o Li spinel. This is in agreement with the chemical analysis (the results of which are shown in Table 2) which indicates that there is a real difference in the composition of samples nominally containing 10 and 46m/o Li spinel. However, as can be seen in Fig. 4iv, the presence of lithium does cause a marked increase in the insulation conductivity above about 20Hz as compared to the pure sialon, data for which were obtained by the same method.

The second region represents a regime in which

$$\sigma_{ac}(ins) = B \exp \left(\frac{-W_{ins}}{kT} \right) \qquad (4-1)$$

where B is a constant. In the exponent, k is Boltzmann's constant and W_{ins} refers to some characteristic activation energy. The values of
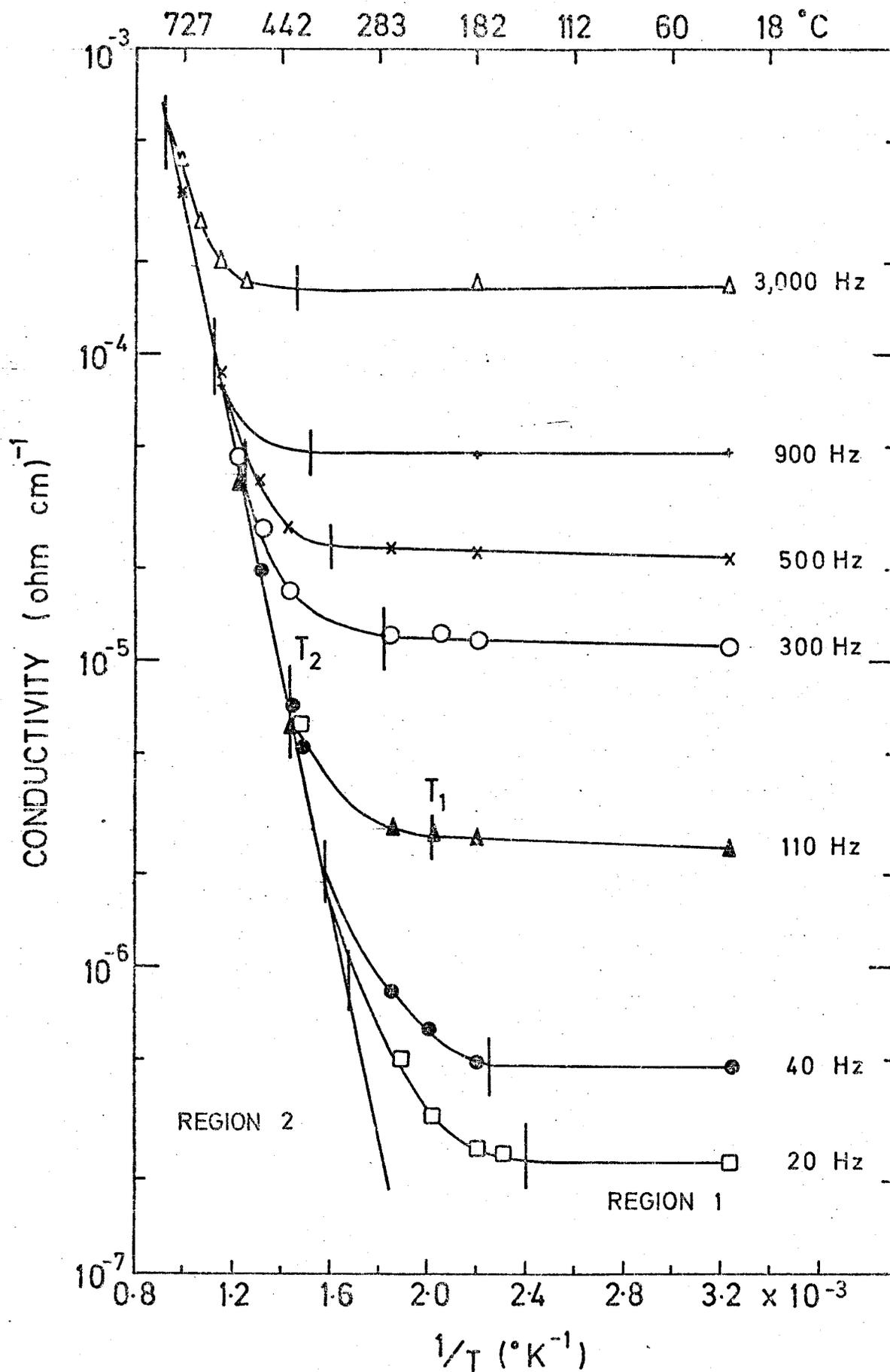
FIG.4iii. The variation of the a.c. insulation conductivity with temperature in a lithium sialon showing the two different conductivity regions.
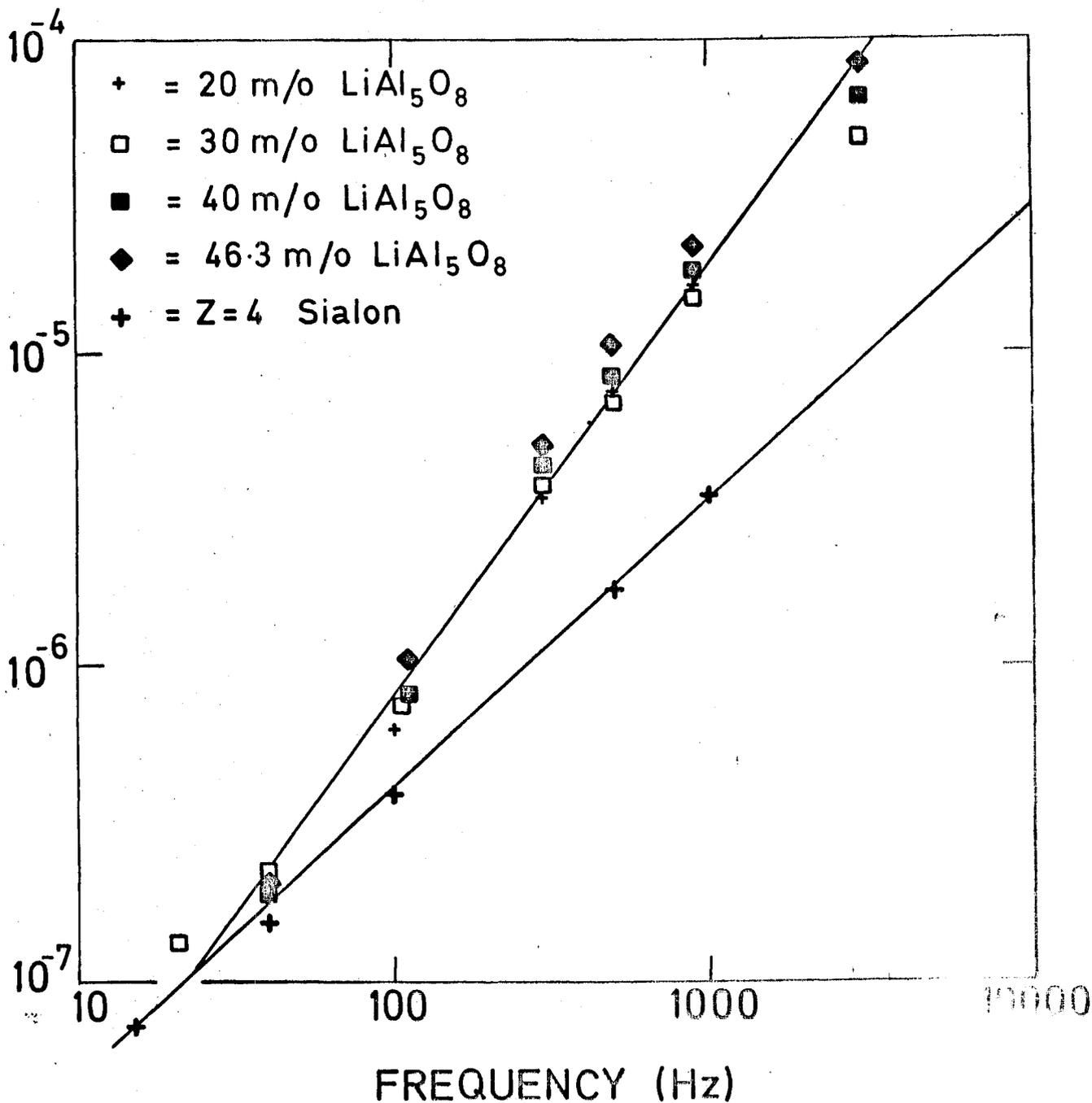
FIG. 4 iv   Comparison   of   the   variation   of   room   temperature
conductivity   with   frequency   of   a   lithium   and   a   pure   sialon.

W_{ins} were computed from least squares fits of equations of the form 4-1 to the data points. The correlation coefficients of these fits were between 0.95 and 0.99 showing that the conductivity closely followed an exponential law in this region of temperature. The values of W_{ins} are shown in Table 3.

It can be seen from Table 3 that all the lithium sialons show similar values of W_{ins}, about 0.7eV; however, there is no correlation between nominal lithium content and activation energy. It is interesting to note that the silicon nitride has a value of W_{ins} of 1.32eV, rather larger than that for the lithium sialons.

It should be noted at this point that errors in the measurements of the sizes of the specimens would have no effect on the determinations of the values of activation energies as these are derived from the slopes of the graphs. The geometrical factor associated with the sample determines the position of the curve relative to the conductivity axis and hence influences only the value of the constant B in equation 4-1. Errors in the measurement of temperature are not systematic and so it is assumed that they will not significantly affect the graph's slope.

The form of the temperature variation of the a.c. insulation conductivity for all sialons (pure, lithium and yttrium) is remarkably similar, as is shown in Figs. 4v and 4vi. Particular interest attaches to the yttrium sialon result since it will be recalled from Chapter 2-4 that the yttrium sialon comprises almost entirely glass which means that the conduction in this material is representative of that in a glassy phase. Since the behaviour of the other sialons is so similar to that shown by the yttrium sample it seems likely that a similar glassy phase must be responsible for the conductivity in all the samples. Hence it is deduced that the glassy matrix surrounding the β' crystallites in the sialons, and in particular in the lithium sialons, is the medium in which the conduction takes place. This is entirely compatible with the microstructure of the sialons as shown in Fig. 2iii since it is the glassy phase which offers the most continuous path through the material.

HIGH TEMPERATURE ACTIVATION ENERGY DATA

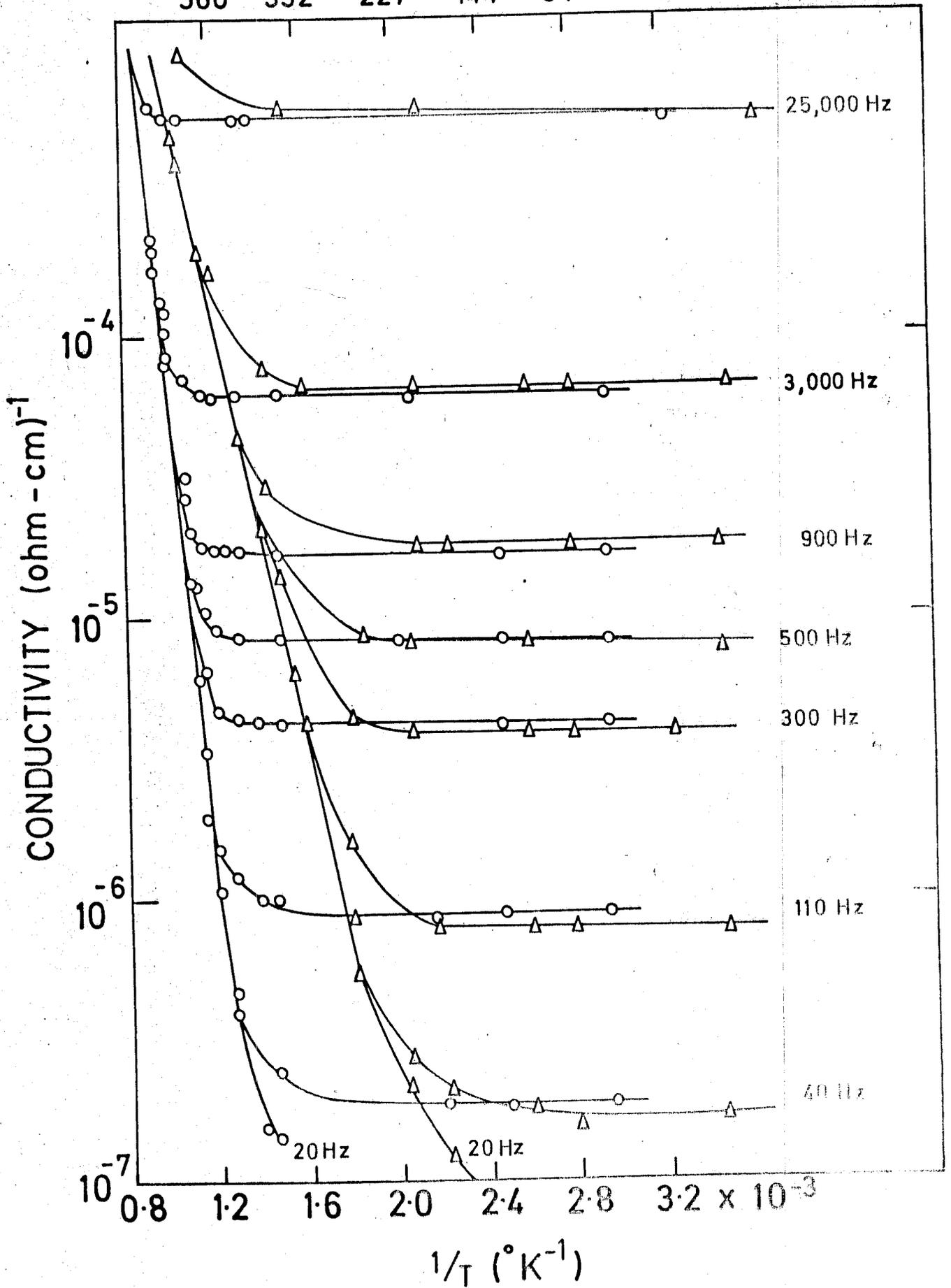| Sample No.	Composition	Li content wt%	W_{ins}(eV)	W_{ac}(eV)	W_{dc}(eV)
1	Si₃N₄	-	1.32		1.37
20	x=4 sialon	-	.677		1.89
21	x=4.8 sialon	-			2.02
Li 30	9.4m/o Li spinel	0.28		.710	.856
Li 7	"				.893
Li 8	"	1.17	.677	.671	.735
Li 22	"		.738		
Li 14	"	1.46	.642		
Li 26	"	1.62	.730		
Li 15	"	1.40	.682	.683	
Li 17	"		2.43		
Y 28	14.3m/o Y₂O₃	-	1.38	1.20	

(Complete details of composition are shown in Table 1)

FIG. 4v Comparison of the variation of the a.c. conductivity with temperature of an Yttria sialon (o) glass and 28 m/o lithium sialon (Δ)

TEMPERATURE °C
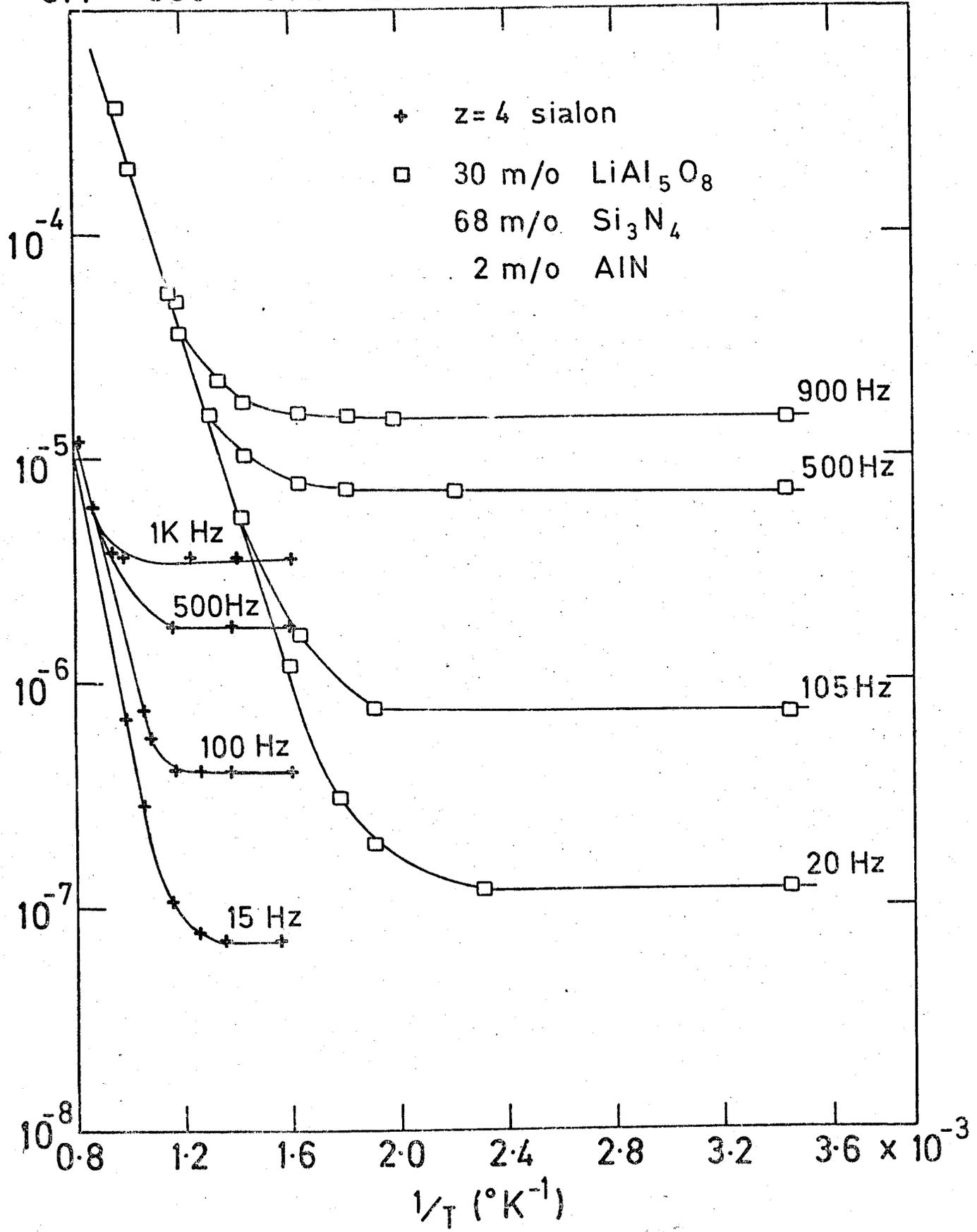
Fig. 6.4vi. Comparison of the variation of a.c. conductivity with temperature of a pure and a lithium sialon.

Legend:
- + $z = 4$ sialon
- □   30 m/o $LiAl_5O_8$
  - 68 m/o Si_3N_4
  - 2 m/o AlN

Curves labelled: 900 Hz, 500 Hz, 1K Hz, 500 Hz, 105 Hz, 100 Hz, 20 Hz, 15 Hz

X-axis: $^1/_T$ $(°K^{-1})$

CHAPTER 5

RESULTS 2 - CONDUCTIVITY MECHANISMS

If it is to be assumed that the glassy content in the lithium sialons is playing a dominant role in determining their conduction characteristics, then the most probable conduction mechanism is hopping. The results presented in the previous chapter strongly suggest that this is so but are not conclusive because the measurements made were of total conductivity whereas a more reliable test can be made by examining the a.c. conductivity using a bridge method. This has been done here and it will be shown in this chapter that all the conductivity behaviour shown by the sialons studied is completely compatible with a hopping mechanism. For convenience the main features of hopping theory are summarised first.

5-1 Theory of Hopping

In the hopping model proposed by Austin and Mott (1969) the charge carriers are electrons, although the mathematical formulation is in terms of polarons, that is electrons and their associated lattice distortion. Polarons are formed when the electron-phonon interaction is strong. There are several types of hopping but the one likely to be most relevant to the sialon glasses involves the electron moving from one localised state to another by an exchange of energy with phonons. The localisation is caused by disorder in the lattice and not by interaction with the phonons.

In such a hopping model the probability per unit time that an electron will jump between two centres with energy levels differing by W_D, the activation energy for hopping due to disorder is proportional to $\exp\left(\frac{-W_D}{kT}\right)$. However in a hopping regime the energy of the polaron, W_H, i.e. the minimised sum of the energies of the electron and the molecule to which it has become temporarily attached, also contributes to the hopping mobility. The combined effect of these two energies yields a d.c. conductivity of the form

$$\sigma_{dc} = D \exp\left(\frac{-W_{dc}}{kT}\right) \qquad (5\text{-}1)$$

where the total activation energy, W_{dc} is given by

$$W_{dc} = W_H + \tfrac{1}{2}W_D \quad \text{for } T > \tfrac{1}{2}\theta_D$$

$$W_{dc} = W_D \qquad \text{for } T < \tfrac{1}{4}\theta_D$$

where θ_D, defined by $\hbar\omega = k\theta_D$, is a temperature characteristic of the average optical frequency ω. In the present work no attempt has been made to deduce the separate contributions made by W_D and W_H to the conductivity as this would have required studying samples at lower temperatures than was possible due to the very low conductivity that the sialons show even at moderate temperatures. The pre-exponential constant, D is the product of terms such that

$$D = D' \exp(-2\alpha a)$$

where D' is a constant determined by the number of electrons able to hop, the number of available sites, the jump frequency and a, the site spacing. The second term is the tunneling factor in which α is the tunneling probability. At lower temperatures the relative importance of W_H and W_D alters and this results in the modified relation

$$\sigma_{dc} = A \exp\left(\frac{-B}{T^{\frac{1}{4}}}\right)$$

where A and B are constants. A fit to this behaviour would be noticeable as a non-linearity in the $\log\sigma_{dc}$ vs $1/T$ plot which would become more pronounced as the temperature was reduced. It may be noted that this type of variation has been reported in several substances in which the conductivity is determined by hopping mechanisms for example in nickel oxide, (Austin and Mott, 1969), and in the chalcedenide glasses, As_2Se_3, (Davis and Shaw, 1970).

As regards the a.c. measurements, one of the salient features of hopping is the occurrence of marked frequency dispersion in the conductivity, σ_{ac}, that is the real part of the conductivity. It is because the theory of hopping has been developed in terms of σ_{ac} that experimentally, bridge methods of measurements of dielectric properties are necessary in order to evaluate the separate components of the conductivity. In the low frequency range (i.e. below about $10^6 Hz$) theory

predicts that at or near room temperature

$$\sigma_{ac} \propto \nu^{0.8} \qquad\qquad (5-2)$$

and Mott and Davis (1968) have shown that two kinds of hopping mechanism can be responsible.   These are

a) transport by carriers excited into localised states at the edges of the valence band

or   b) hopping by carriers with energies near to the Fermi level, provided that $N(E_F)$ is finite.

The two processes can be distinguished by investigating the frequency dependence of the conductivity in the temperature region at which frequency dispersion occurs.   If case a) applies then there will exist a threshold frequency below which there is no dispersion and $\sigma_{ac} = \sigma_{dc}$. Above the threshold frequency the conductivity varies with frequency according to equation 5-2.   This behaviour corresponds to a multiple hopping regime.   If, alternatively, σ_{ac} is weakly dependent on temperature and the frequency dispersion represented by equation 5-2 occurs from the lowest frequencies then case b) applies.

Hopping conductivity theory also predicts the form in which the dielectric constant, ε', and the loss tangent, $\tan\delta$, should vary with frequency at room temperature.   The criteria for hopping to occur in a material are that both ε' and $\tan\delta$ should be virtually independent of frequency and that if they do show some slight variation with the frequency they should do so in the same sense.   This affords a unique method of distinguishing hopping from other mechanisms since in materials where, for example, the Maxwell-Wagner model applies ε' and $\tan\delta$ will vary with frequency in opposite senses.   There appears to be no well developed theory for the temperature variation of ε' and $\tan\delta$ in hopping materials but there is some evidence, discussed later, to suggest that both rise as the temperature increases.

5-2 D.C. Results

The d.c. conductivities measured as described in Chapter 3-3-2, are

shown for three different lithium sialons in Figs. 5i,ii,iii and are plotted as log σ_{dc} vs $(T^{\circ}K)^{-1}$. These plots yielded straight lines from the maximum temperature reached down to at least $200^{\circ}C$ representing a relation of the form shown in Equation 5-1. The values of W_{dc}, the d.c. activation energy were derived from the slopes of the plots and are shown in Table 3. It will be noticed that although only three values for lithium sialons are available it is clear that there is no correlation between activation energy and starting composition, this confirms the trend observed in the case of the insulation conductivity. However, it is noticeable that W_{dc} is approximately constant for the three samples, although the lithium contents determined by analysis differed by a factor of three (Table 2). The d.c. results suggest that a value near 0.8eV may be taken to correspond to an activation energy associated with the presence of lithium. This suggestion is supported by the results of W_{dc} for silicon nitride and the two pure sialons for which the values of W_{dc} are all much larger and the comparison indicates that the experimental method can genuinely distinguish marked changes in activation energy.

As mentioned in the previous section the change of temperature dependence to the $T^{-\frac{1}{4}}$ law should cause a deviation from the linear behaviour shown by the conductivity (as displayed in Figs. 5i,ii,iii) at the low end of the temperature scale. There is some evidence for a departure from linearity in each of the samples. However, this area of the graph corresponds to the situation in which the conductivity measuring apparatus was being used at maximum sensitivity and hence errors on these measurements are likely to be greater than those taken at higher temperatures. Precise measurements at lower temperatures with more sensitive equipment would be necessary to establish the $T^{-\frac{1}{4}}$ dependence convincingly. Most materials which show this behaviour, e.g. NiO (Austin and Mott, 1969) do so at temperatures of the order of $50^{\circ}K$. However, the overall d.c. behaviour of the lithium sialons is completely consistant with a hopping model of conduction.
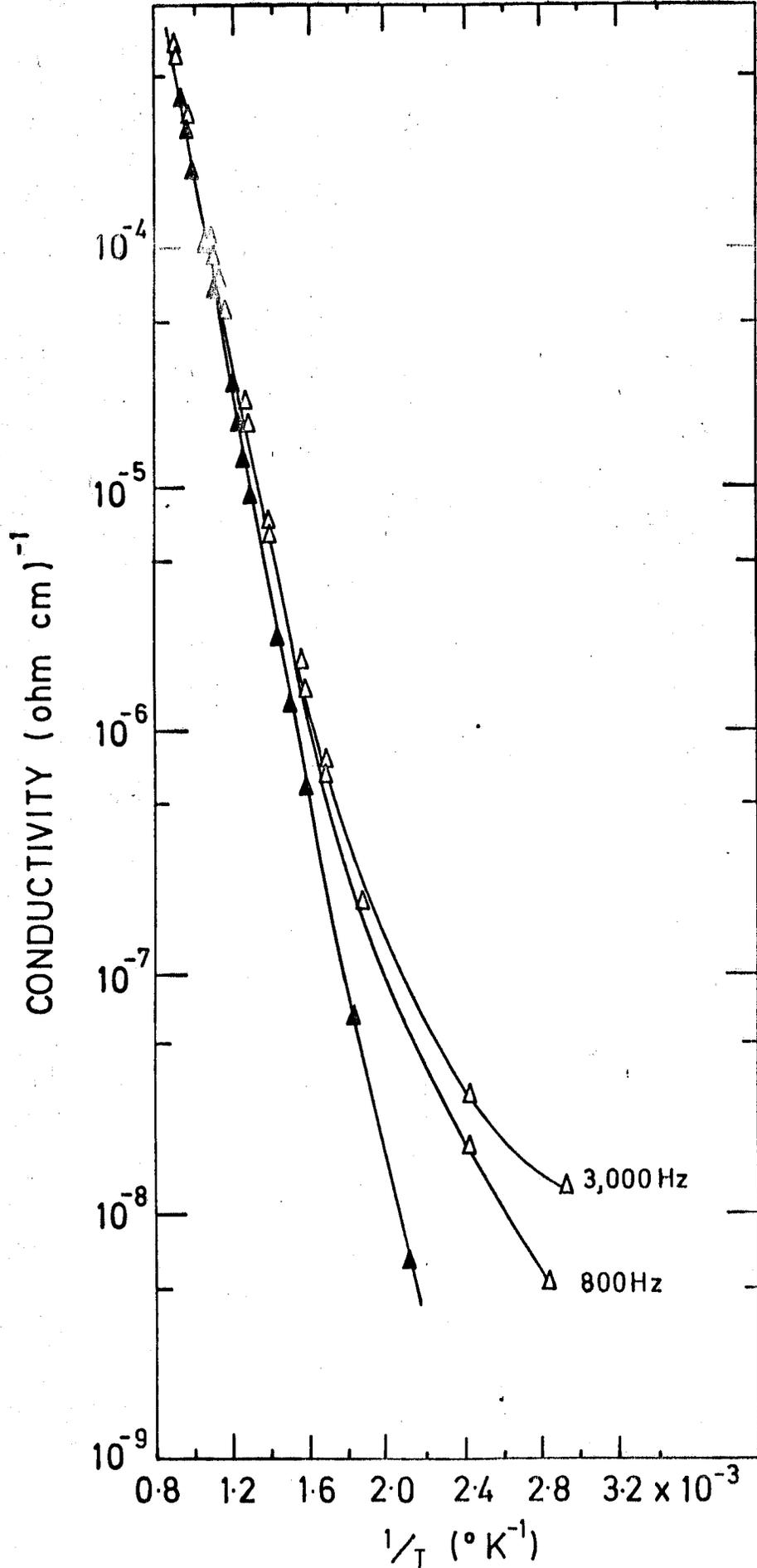
FIG. 5i   The a.c. (△) and d.c. (▲) conductivities in 9·4 m/o $LiAl_5O_8$, 85·3 m/o Si_3N_4, 5·3 m/o Al_3O_3N as a function of temperature.

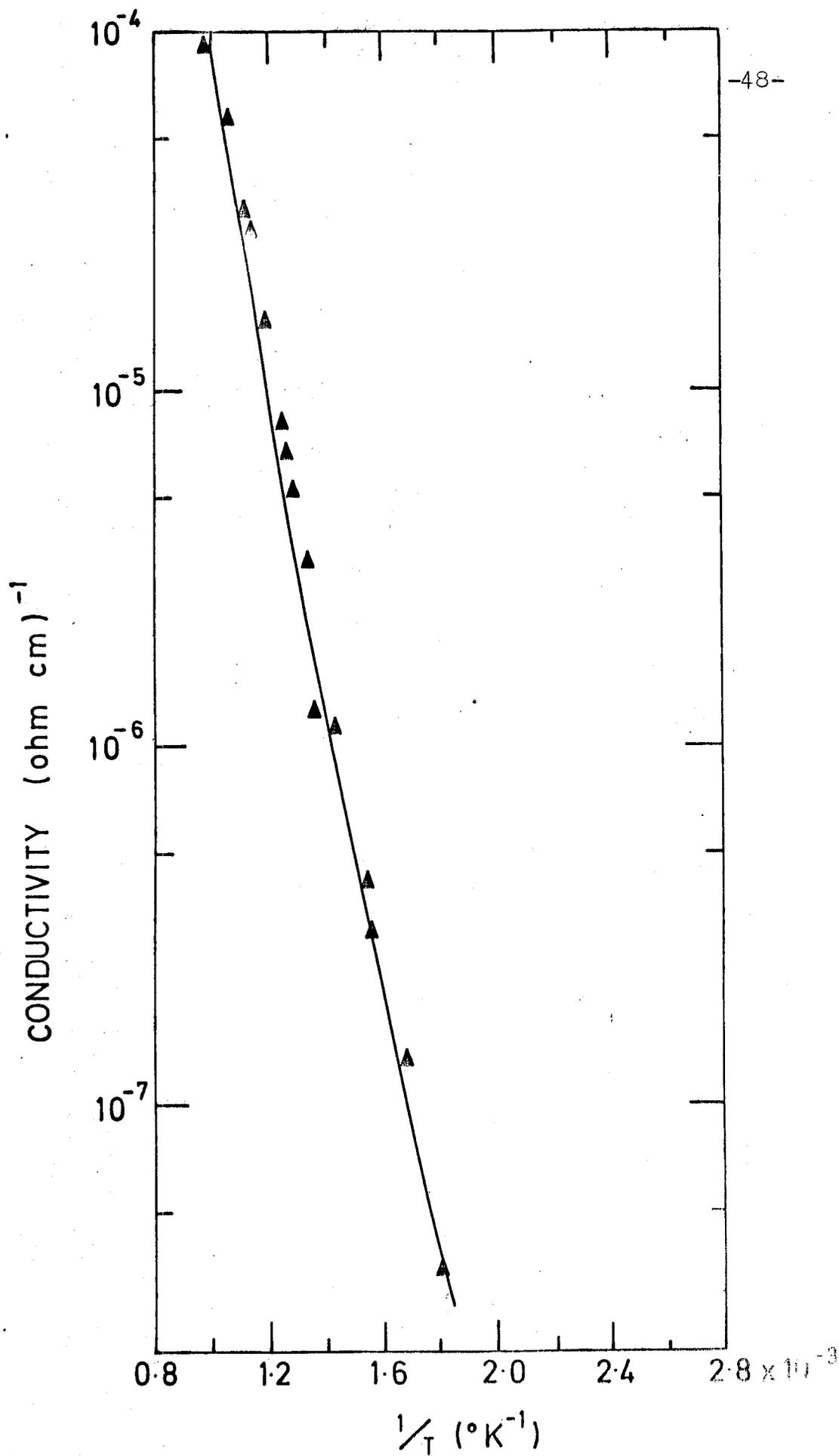FIG. 5 ii   The variation of d.c. conductivity
with temperature in 20 m/o Li   sialon.
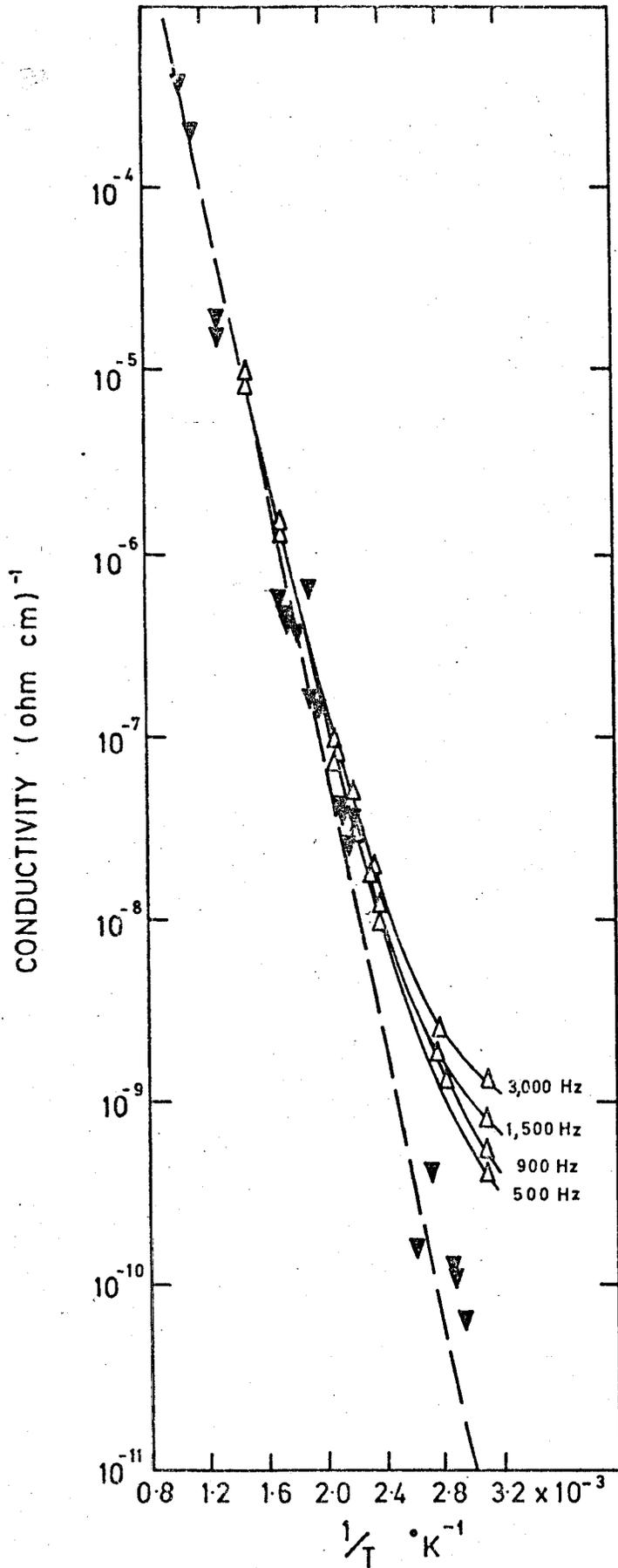
FIG. 5iii. The a.c. (Δ) and d.c. (▼) conductivities in 28 m/o LiAl₅O₈ , 63 m/o Si₃N₄ , 9 m/o AlN as a function of temperature.

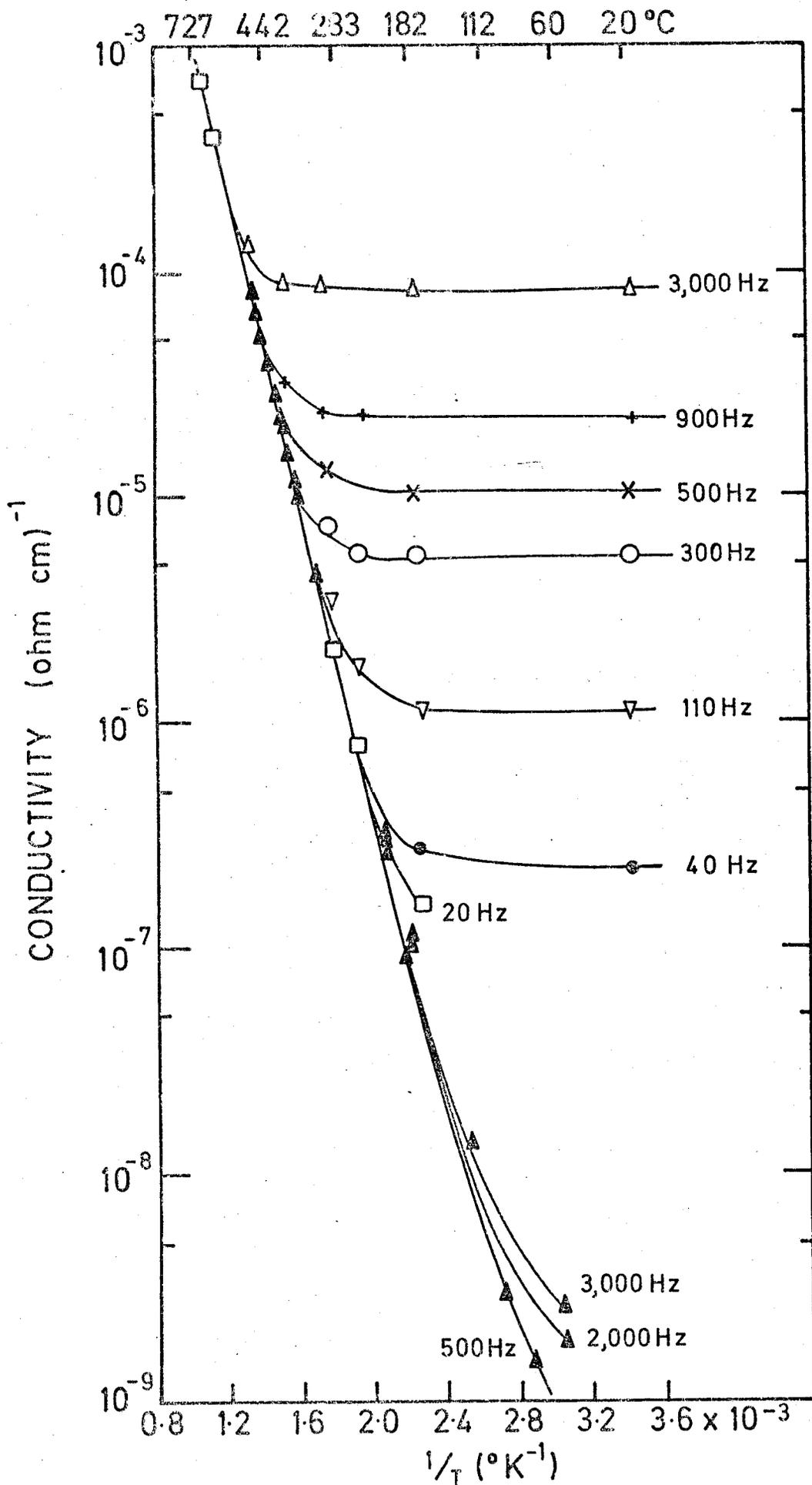FIG. 5iv The a.c. (▲) and a.c. insulation conductivity as a function of temperature in 46·3 m/o Li spinel sialon.

It would be valuable to obtain optical data on the samples represented in Figs. 5i,ii,iii in order to investigate further the value of the activation energy W_{DC}. As can be seen from Table 3, a typical value is 0.8eV, equivalent to a wavelength of 15,529Å. At this wavelength or a multiple of it there should exist a band edge corresponding to increased absorption as the energy of the incoming photon is great enough to cause an electron to hop. The exact position and details of the band-edge would yield useful information on the conduction mechanism. However, unfortunately 15,529Å represented a gap in the wavelength range that was available on the spectrophotometers; nor is there any published optical data. Optical results that have been obtained are shown in Appendix 2 to this thesis.

5-3 A.C. Results

The a.c. conductivity, as measured and discussed in Chapter 3-3-2, shows two regions in its temperature dependence. This was not unexpected since the a.c. insulation conductivity also showed two very distict conductivity regimes. However the behaviour reported here is significantly different. Figs. 5i,iii,iv show the a.c. conductivity as a function of reciprocal temperature for three lithium sialons. In the high temperature region the a.c. conductivity, σ_{ac}, is superimposed on the a.c. and d.c. insulation conductivities (the values of the activation energies are given in Table 3). At more moderate temperatures σ_{ac} shows a region of frequency dispersion. To establish the nature of the frequency dispersion, the data points shown on Figs. 5i,iii,iv in the frequency dispersive regions of the graphs were replotted in the form of log frequency vs log conductivity. The data from Fig. 5iii as replotted is shown in Fig. 5v.

In order to obtain reliable frequency dispersion data at temperatures below about 70°C it was necessary to use the jig shown in Fig. 3ii with samples having gold evaporated contacts so that the effect of stray conductances and capacitances could be evaluated and then allowed for in deriving the results. This was done for a sample of 40m/o Li spinel,
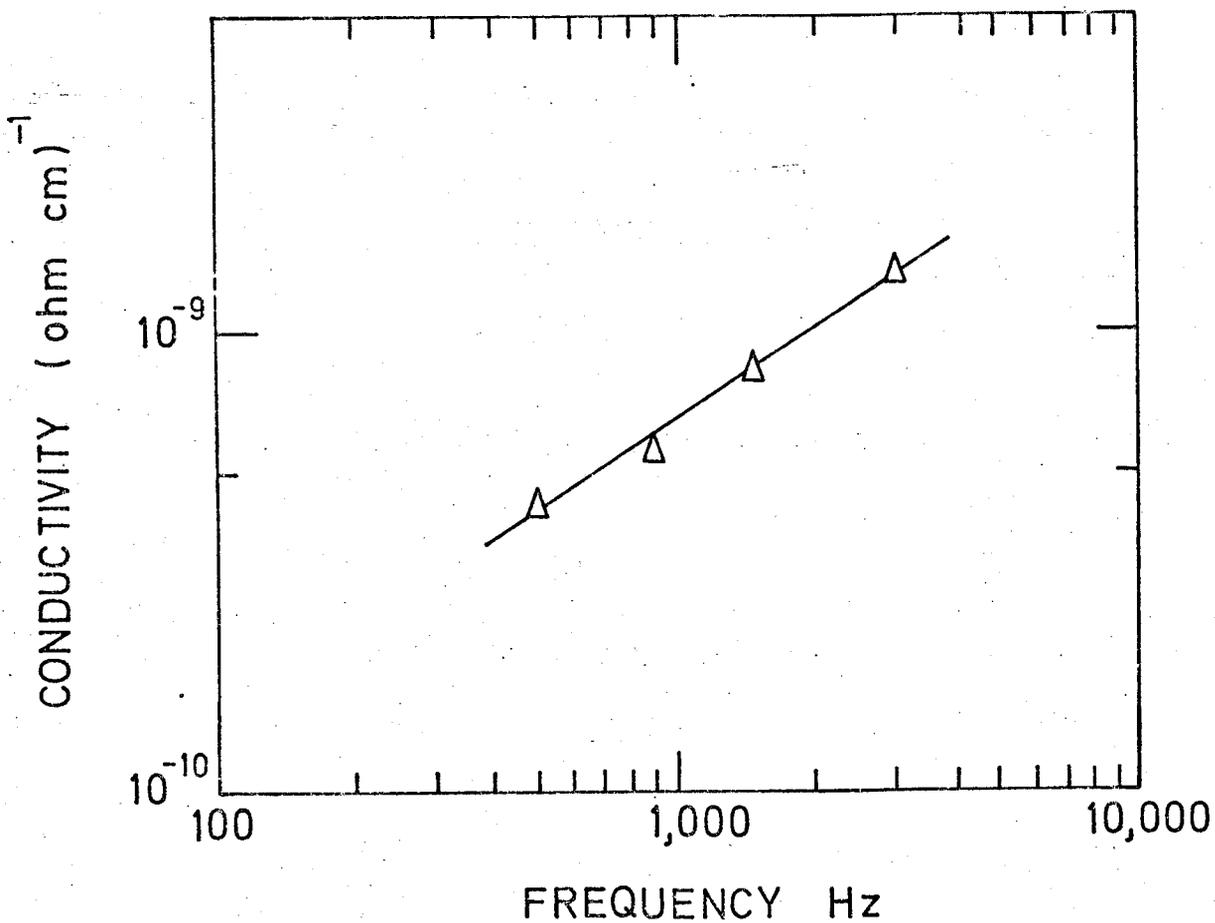
FIG. 5v The a.c. conductivity as a function of frequency at 50°C in 28·3 m/o $LiAl_5O_8$, 62·3 m/o Si_3N, 9·3 m/o AlN.

60m/o silicon nitride and the log σ_{ac} vs log frequency characteristic is shown in Fig. 5vi. This represents the best data available in the frequency dispersive region. Fig. 5vi yields a value of 0.69 for s at 20°C, with a correlation coefficient of 0.9995 for a linear fit.

5-4 Discussion on Conductivity

Some comment may first be made on the magniturdes of the conductivities observed. At 100°C the d.c. value of the conductivity is about 10^{-10} (ohm cm)$^{-1}$ and this rises to around 10^{-3} (ohm cm)$^{-1}$ at 700°C. There does appear to be some dependence of σ_{dc} on lithium content; for example at 350°C the values of σ_{dc} are 2.10^{-6} and 5.10^{-7} respectively for specimens containing 28 and 9.4 m/o Li spinel, corresponding to 1.0 & .3wt% Li as determined by chemical analysis. The same trend is clear from comparison of the a.c. data at corresponding temperatures and frequencies. A major conclusion, discussed more fully in the following chapter, is that in general terms the conductivities of the lithium sialons are, at elevated temperatures much greater than those reported for pure sialons (Thorp and Sharif, 1976); it is reasonable to attribute this to the inclusion of lithium. In this respect it may be significant that the single sodium sialon available for examination also gave conductivities (Fig. 4i) ranging from 4×10^{-9} at 330°C to 1.5×10^{-4} (ohm cm)$^{-1}$ at 700°C, i.e. roughly the same conductivity range as observed for the lithium sialons.

At high temperatures the a.c. and d.c. conductivities are superimposed; this implies that in this region the same mechanism is responsible for both. The exponential shape of the temperature dependence does not in itself indicate which that mechanism is since ionic, electronic, semiconducting and hopping conduction all give this behaviour. The activation energy of 0.8eV is large but the same for all the lithium sialons. The fact that the activation energy obtained from the slope of the a.c. conductivity (W_{ac}) is somewhat lower than for the d.c. case is probably due to the residual effect of the frequency dispersive region of the curve.
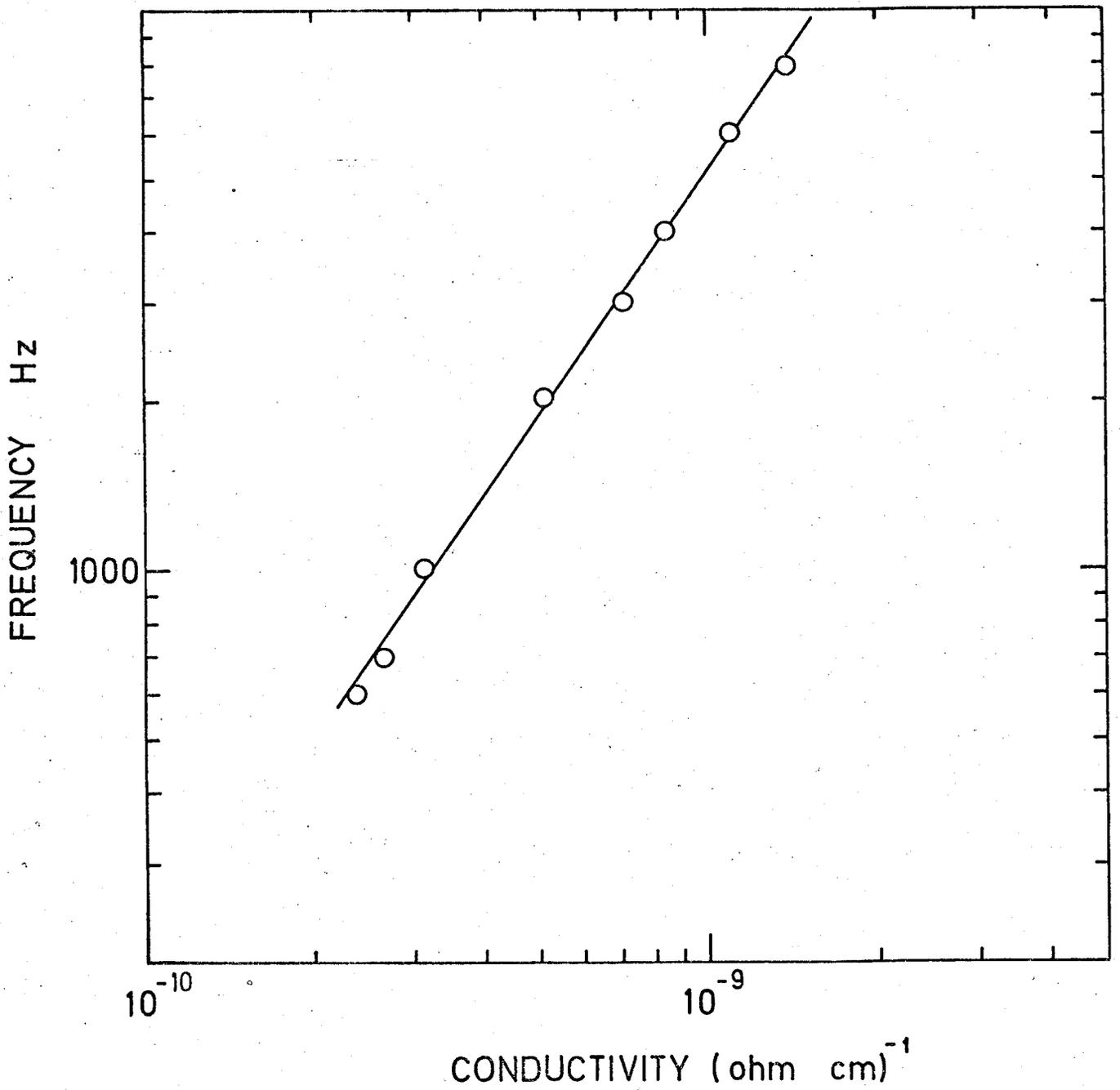
FIG. 5 vi.   The variation of the a.c. conductivity with frequency at 20°C in 40 m/o $LiAl_5O_8$, 60 m/o Si_3N_4.

In all the cases the activation energy was obtained using a least squares fit to the points in the exponential region.

The a.c. results provide direct evidence for hopping at the lower temperatures investigated in that σ_{ac} enters a region of frequency dispersion as the temperature is decreased. For data taken near room temperature there is resonably close agreement with a σ_{ac} $v^{0.8}$ law and furthermore the frequency dispersion appears to begin from the lowest frequencies, (20Hz) at which measurements were made. These observations fulfil the criteria summarised in Section 5-1 and indicate that in this temperature regime the conductivity mechanism is hopping by carriers with energies near to the Fermi level.

5-5 Dielectric Constant and Loss Results

The values of two dielectric functions, the dielectric constant, ε' and the dielectric loss, tanδ were computed from the values of the conductance and parallel capacitance, measured using the Wayne-Kerr bridge as described in Chapter 3-3-2.

Consider first the room temperature data since it is in this temperature region that electron hopping appears to dominate. For the reasons discussed in Chapter 3-3-2 this was obtained using the jig shown in Fig. 3ii. Fig. 5vii (a+b) shows the frequency dependence of the dielectric constant and loss at room temperature for a sample containing 40m/o Li spinel. The value of ε' at the lowest frequency of measurement (500Hz) was 11.5 and there was a decrease to 11.0 at 3kHz; thereafter ε' remained substantially constant up to the highest fequency of measurement, 8kHz. The tanδ variation shows a similar trend in that there is a noticeable decrease, from 0.07 to 0.04, between 500Hz and 3kHz and then a more gradual fall resulting in a value of 0.03 at 8kHz. The significant fact is that both the dielectric constant and loss variations occur in the same sense giving additional evidence for the validity of the hopping model in this temperature region. All the lithium sialons showed very similar results. The relatively high values of tanδ show
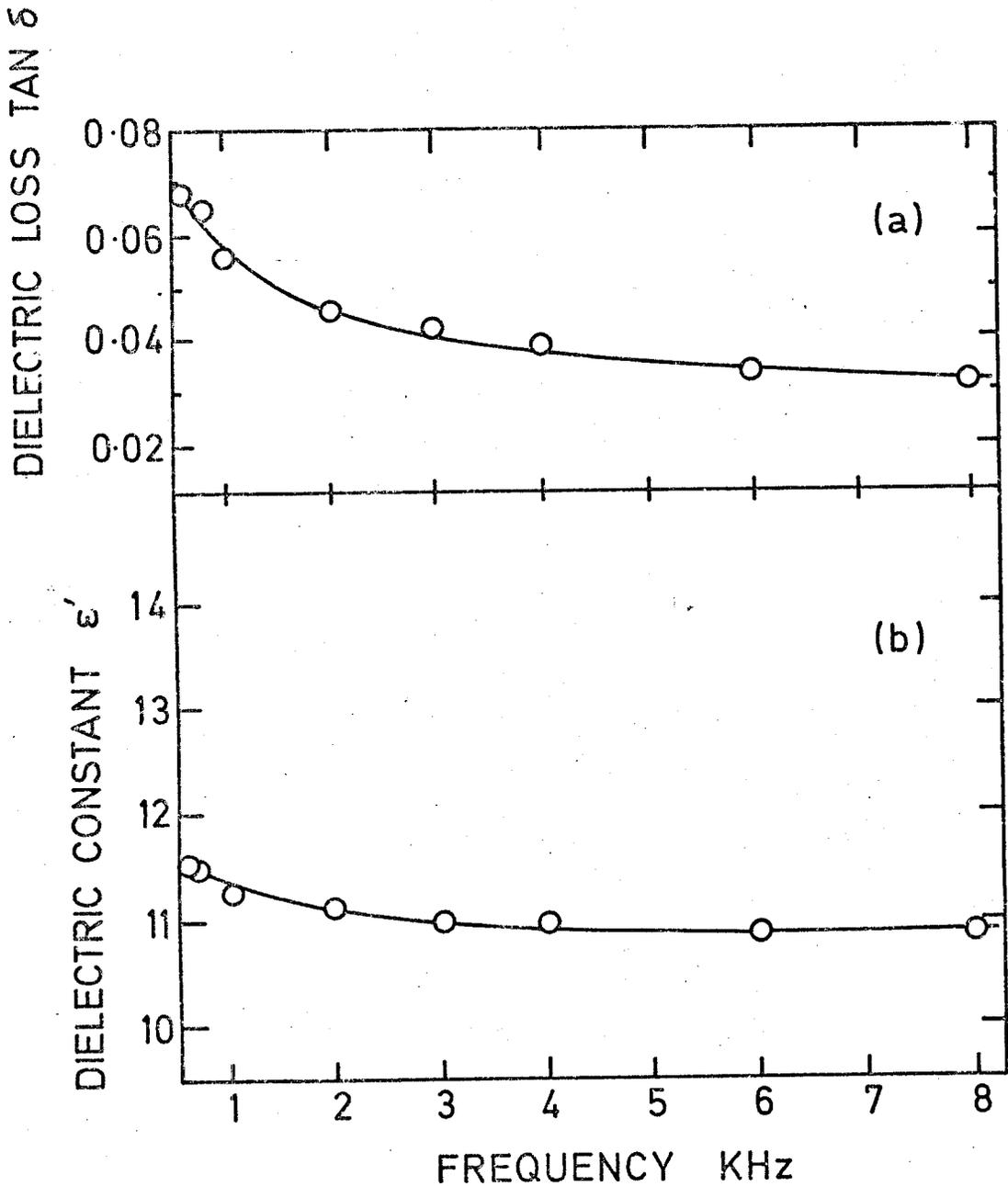
FIG.5vii The dielectric loss and constant vs frequency at 20°C for the sample of 40 m/o $LiAl_5O_8$, 60 m/o Si_3N_4

again that even at room temperature the lithium sialons are not very good insulators, for which a value of tanδ nearer to .001 or less would have been found.

At higher temperatures electron hopping is no longer the dominant mechanism, two other effects which are likely to be of major importance are contributions from electron or hole conductivity via the conduction band or from ionic conduction. Hence a considerable amount of information was obtained from studying the temperature variation of both ε' and tanδ. Experimentally this aspect of the measurements posed problems in that the jig used for the room temperature work would not have been suitable; the insulating teflon rods quickly lost their high relative resistance as the temperature increased and it was felt that there might have been a risk of gold diffusing into the sample. It was therefore necessary to use platinum paste electrodes baked onto the sample which was then simply suspended by platinum wires inside the furnace. The implicit assumption that platinum, having a larger ionic radius than gold, would be unlikely to diffuse appreciably was sustantiated by the lack of evidence for platinum in the X-ray powder photographs taken in connection with the decay of the d.c. insulation resistance.

The results shown in Fig. 5viii, which refers to the 9.4m/o Li spinel sialon, illustrates the general features observed. Both ε' and tanδ are temperature dependent though at any given temperature the forms of both ε'-ν and the tanδ-ν variations are similar to their room temperature counterparts, i.e. the major decreases in ε' and tanδ occur in the lower frequency range. The magnitudes of the temperature dependencies are striking. At lkHz tanδ rises from about 0.06 at room temperature to nearly 10 at 770°C, a change of approximately three orders of magnitude; in ε' the rise is from 11 at room temperature to 5×10^4 at 770°C. (In view of the very high values of ε' recorded the measurement technique was critically reviewed and tests were made in the open-circuit situation without a sample present to find whether any spurious capacitances were
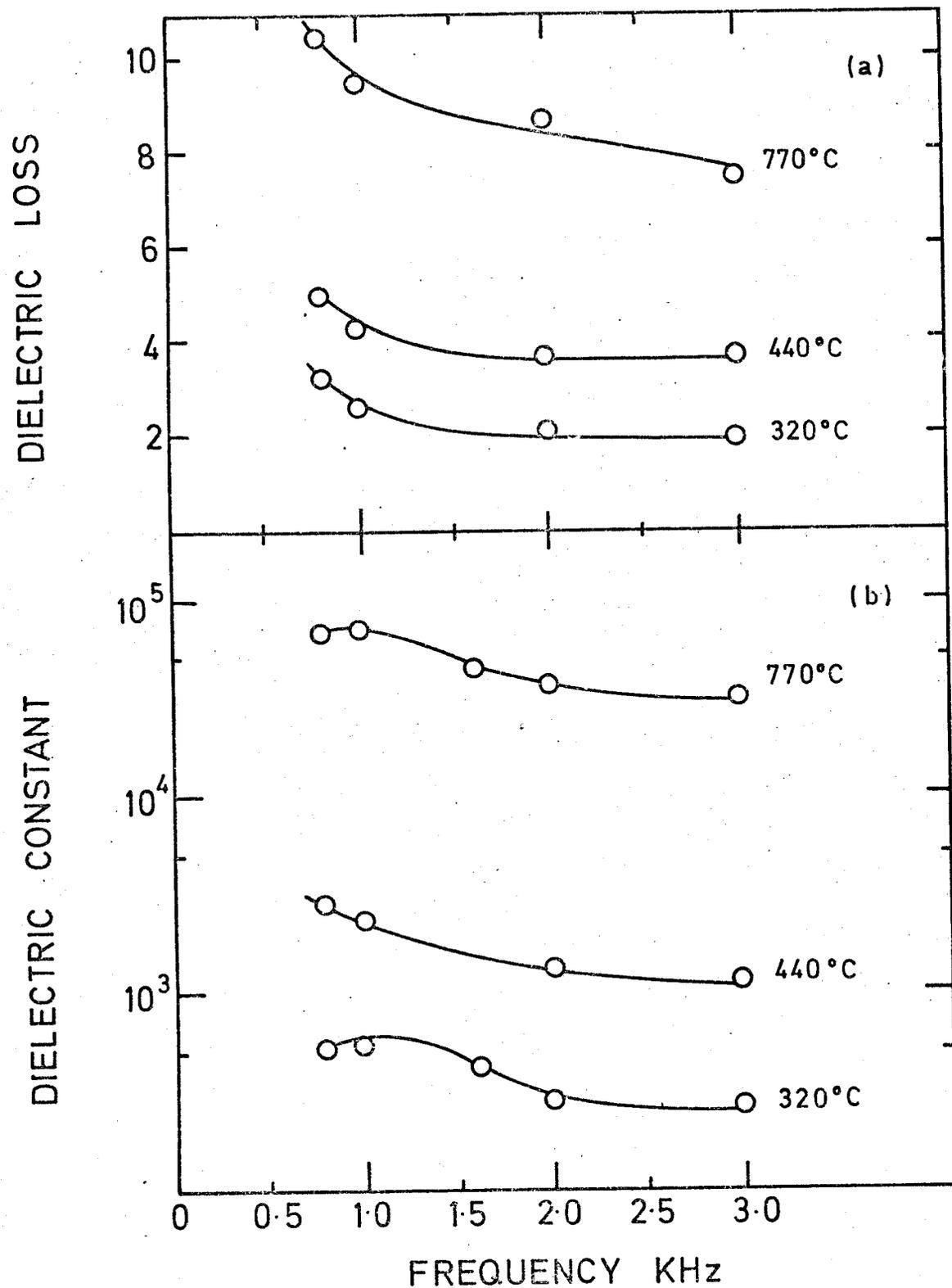
FIG. 5viii   The   dielectric   loss   and   constant   vs frequency   at   different   temperatures   in   a   sample of   9·4 m/o LiAl$_5$O$_8$,   85·3 m/o   Si$_3$N$_4$,   5·3 m/o   Al$_3$O$_3$N.

being introduced at high temperatures; these tests proved negative so it
is felt that there is no reason to doubt the values of ε' or tanδ recorded).
Further data for the sample containing 28.4m/o Li spinel is given in Fig.5ix
which indicates rather more clearly a trend detectable in the previous
figure, namely that the increase in tanδ per unit temperature rise is more
pronounced at lower frequencies than at higher ones.   Since the 9.4m/o
and the 28.4m/o Li spinel sialons were, on analysis, found to be of
genuinely different chemical composition, the data shown in Figs. 5viii
and ix can be used to assess whether the temperature variations are depen-
dent on composition.   A comparison of data for samples containing sig-
nificantly different amounts of lithium is shown in Table 4;   these
results refer to a frequency of 1.5kHz.   It can be seen that the sample
with the higher lithium content gives the larger high temperature values
of both ε' and tanδ but because of the associated changes in the aluminium
and silicon contents this evidence alone is insufficient to enable lithium
to be isolated as the sole cause of the change.

Turning now to the reasons for the temperature variations of the di-
electric constant and loss which are similar to the rapid increase in
these parameters that is found in many ceramics and glasses.   Some of
these phenomena are reviewed by Kingery (1960).   At frequencies below
about 10^6Hz (i.e. the frequency range considered in the present work) the
major losses in dielectrics arise from electronic or ionic conduction,
that is increases in carrier density in the conduction band, or from dipole
relaxation losses due to ions.   Dipole relaxation refers to the process
in which an ion oscillates between two equivalent ion positions. Both
these two processes cause the dielectric losses to increase at low fre-
quencies and as the temperature is raised; at moderate frequencies dipole
relaxation is often the major contributor to the losses.   One of the
effects of this is that, for many insulators, tanδ increases exponentially
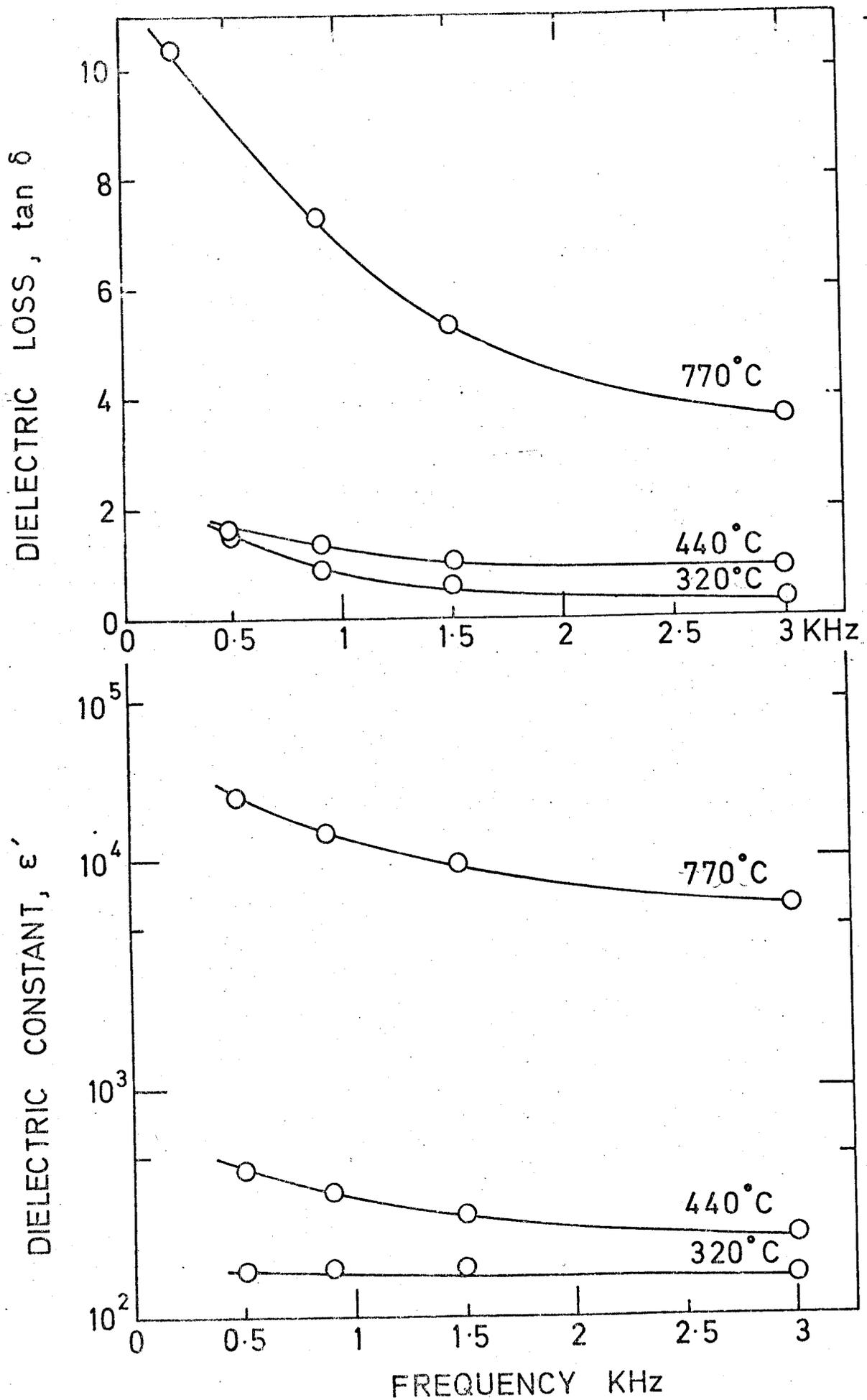with temperature; an example of this is shown by a lithium sialon in
Fig. 5x.

FIG. 5ix The dielectric loss and constant vs frequency at different temperatures in 28·4 m/o $LiAl_5O_8$, 62·3 m/o Si_3N_4, 9·3 m/o AlN.

TABLE 4

COMPARISON OF 1.5kHz DATA FOR SAMPLES OF DIFFERENT LITHIUM CONTENT

Analysis	ε'		$\tan\delta$	
	20°C	440°C	20°C	440°C
9.4m/o Li spinel				
Al Si Li				
11 42 0.3wt%	11	1,500	0.05	4
28.4m/o Li spinel				
Al Si Li				
23 28 0.9wt%	11	10,000	0.05	6
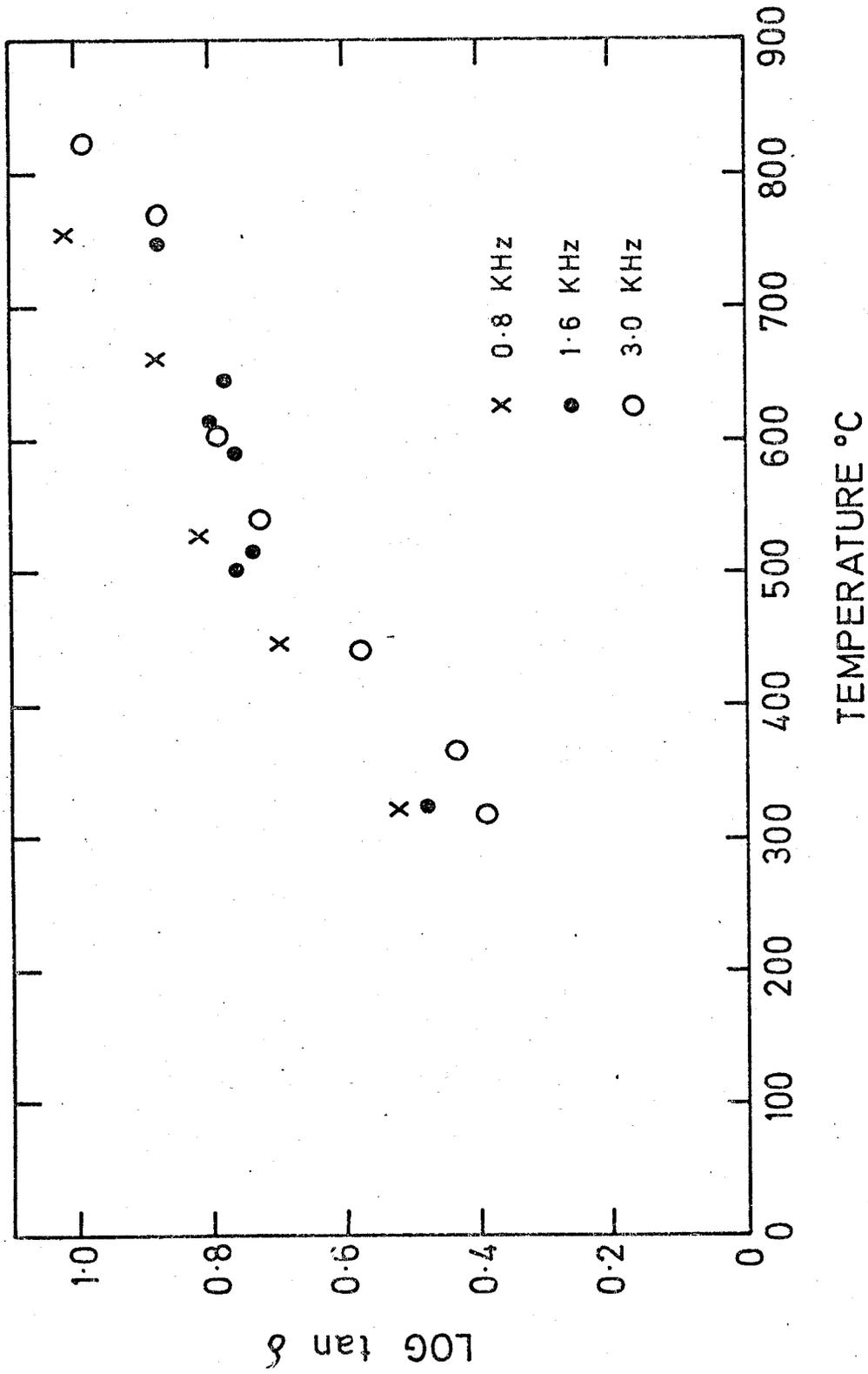
FIG. 5x   Variation of dielectric loss as a function of temperature
in 9·4 m/o LiAl₅O₈ , 85·3 m/o Si₃N₄ , 5·3 m/o Al₃O₃N

In the case of a dipole relaxation process in which the relaxation time is τ the maximum energy loss will occur at a frequency ω equal to the relaxation frequency τ that is when $\omega\tau=1$. This corresponds to a loss peak on a tanδ vs frequency plot. As the relaxation frequency increases exponentially with temperature the position of the maximum of the loss peak will move to higher frequencies as the temperature is raised. Thus by considering the variation of tanδ with frequency it should be possible to find if ion relaxation is present. Over the frequency and temperature ranges investigated there was no evidence for loss peaks.

A second reason for the rapid increase in the dielectric constant and loss is that space charge polarisation effects are playing an important role especially as the temperature is increased. Such effects are a common feature of ceramics which are polycrystalline and polyphase. The probability is that the two (or more) phases will have different electrical characteristics, that is the electrical conductivity of one of the phases will be higher than that of the other; in this context the phase boundary can be thought of as a second phase in that its electrical properties will be different from those of the crystal. The motion of the charge carriers occurs readily through one layer but it is interrupted when it meets a phase boundary. This results in the build-up of charge at the interface. This is measured as a high dielectric constant since by definition the dielectric constant is a measure of the charging effect on the material caused by the applied electrical potential.

In the sialons the picture is not so simple as a layer model would suggest since as will be recalled from Chapter 2 the sialon crystallites are surrounded by the glassy phase giving a somewhat more complex structure but the general argument above is still valid. If this effect is important in explaining the rapid rise in ε' and tanδ it implies that the difference in the conductivities of the two phases itself increases which

further implies that one or other of the conductivities must increase
at an even greater rate; it is generally true that the conductivity
increases with temperature whatever the mechanism involved maybe.
This is further evidence of the importance of the glassy phase in de-
termining the value of the conductivity in the lithium sialons since if
most of the conductivity is being provided by only one phase then from
the micro-structural data that is available from Fig. 2iii the glassy
phase is the only contender.

CHAPTER 6

COMPARISON WITH OTHER MATERIALS

In the two previous chapters, the data obtained on the electrical properties of a series of lithium sialons has been reported. In conclusion, it is interesting to make a comparison between their properties with those of other materials examined by the same or similar techniques. The comparisons made here are with pure sialons and with the yttrium sialon glass thought to be similar in nature to the glassy phase in the lithium sialons investigated.

6-1 Comparison with Pure Sialons

Most of the data presented in this section is taken from published (Thorp and Sharif, 1976) or recent, unpublished work by R.I. Sharif.

The insulation conductivity of the pure sialons may be summarised as follows, taking a z=4 sialon as an example. Under d.c. conditions the conductivity, σ_{dc} is less than 10^{-10} (ohm cm)$^{-1}$ at room temperature and rises according to

$$\sigma_{dc} = A \exp\left\{\frac{-B}{T^{\frac{1}{4}}}\right\}$$

up to about 700°C at which temperature $\sigma_{dc} - 10^{-7}$ (ohm cm)$^{-1}$. Above 700°C the variation changes to

$$\sigma_{dc} = A \exp\left\{\frac{-W_{dc}}{kT}\right\}$$

and this continues up to the highest temperature (1,000°C) at which measurements were made. At 1,000°C, $\sigma_{dc}=4\times10^{-6}$ (ohm cm)$^{-1}$. In the high temperature region the slope of the log σ_{dc} vs 1/T plot yielded an activation energy, W_{dc} of 1.64eV. In the pure sialons there is no evidence for degradation occurring when a d.c. voltage is applied and hence there is no difference for this material between the d.c. insulation conductivity and the d.c. conductivity measured using low voltages as described in Chapter 3-3-2.

As regards the a.c. insulation conductivity over the same temperature ranges, it was found that

a) at high temperatures log $\sigma \propto 1/T$ indicating behaviour very similar to that found in the d.c. case but with an associated activation energy of 1.32eV; this behaviour was independent of frequency

b) at lower temperatures, that is below about 700°C the conductivity became strongly frequency dependent and as the temperature dropped, almost independent of temperature.

Comparison of these results with those for the lithium sialons shows that

i) degradation under d.c. voltages occurs in the lithium sialons but not in the pure sialons

ii) at high temperatures the d.c. conductivities show similar behaviour but below 700°C the pure sialons deviate from an exponential relationship between log conductivity and reciprocal temperature whereas the lithium sialons showed no definite proof of this

iii) the general form of the a.c. insulation conductivity was very similar and could be divided in both cases into a 'high temperature regime' and a 'low temperature regime'

iv) the change over temperature from high to low temperature behaviour is much higher in the pure sialons (700°C as compared to 450°C in the lithium sialons)

v) the values of the room temperature insulation conductivity are similar in both types of material but at higher temperatures, i.e. those in the exponential region the conductivity of the pure sialons is at least two orders of magnitude less than that of the lithium doped samples (Fig. 4vi): an even greater difference is to be seen in the d.c. conductivities, e.g. at 550°C σ_{dc} (pure sialon) = 10^{-9} (ohm cm)$^{-1}$ as compared to σ_{dc}(28m/o Li spinel) = 10^{-4} (ohm cm)$^{-1}$

vi) in the low temperature region, using the Wayne-Kerr bridge, both materials showed frequency dispersion such that $\sigma_{ac} = A\omega^s$ where

s = 0.7 for lithium sialons and 0.9 for pure sialons

vii) the activation energy corresponding to the exponential part
of the conductivity/reciprocal temperature plot is less in the case of
lithium sialons, 0.7eV compared to a value of 1.32eV for the pure sialon.

The similarity in the general features of the behaviour between pure
and lithium sialons suggests that similar conductivity mechanisms apply
to both classes of materials.   At the lower end of the temperature
scale both appear to show the characteristics of a hopping model which,
as mentioned earlier is entirely consistent with the presence of a glassy
phase in the materials.   The addition of lithium increases the conduct-
ivity and this not only implies a very considerable increase in the
number of carriers available but also suggests that the reduction in change-
over temperature between the two conductivity regimes may be attributable
to a simultaneous increase in the number of impurity levels produced.

Further evidence for a hopping model is given by an examination of
recently obtained dielectric data (Sharif, unpublished).   Firstly con-
sider the form of the variations with frequency of ε' and $\tan\delta$ at room
temperature, Fig. 6i.   The values observed at 200Hz are $\varepsilon' \simeq 10$, $\tan\delta \simeq$
7×10^{-3}, between 200Hz and about 10^6Hz both are nearly independent of
frequency;   above 10^6Hz (a frequency range beyond that employed for the
studies on lithium sialons described earlier) there is a marked rise in
both ε' and $\tan\delta$.   At the low and mid frequencies the form of the vari-
ation is very similar to that found with the lithium sialons but it is
noticeable that the loss ($\tan\delta$) is greater at any particular frequency
for the lithium sialon whereas ε' is roughly the same.

The temperature variations of ε' and $\tan\delta$, examined independently by
R.I. Sharif, make an important comparison to the data reported in the
previous chapter.   His results for z=3.2 sialon are reproduced in Figs.6ii
(a + b).   These show that ε' is both frequency and temperature dependent
above about 300°C.   The greatest effect occurs at the lowest frequency,
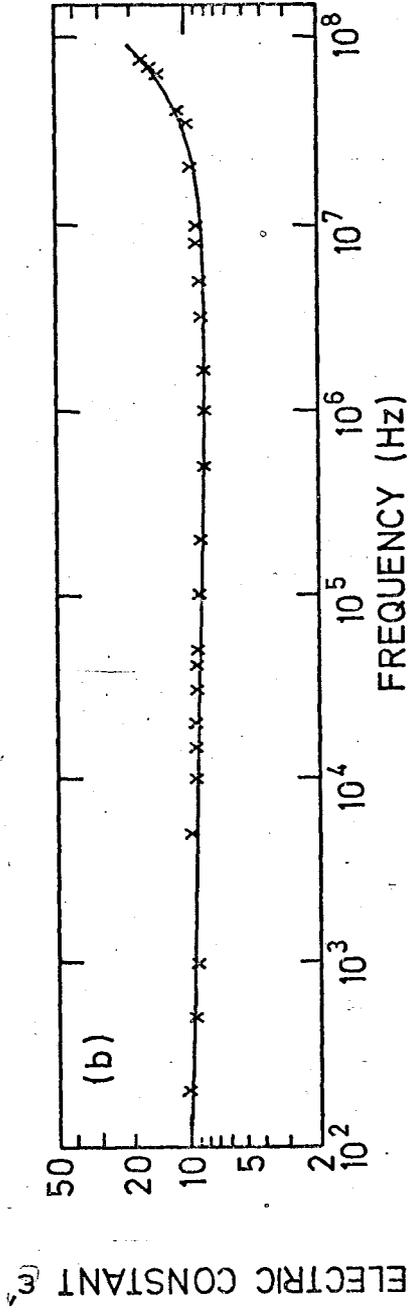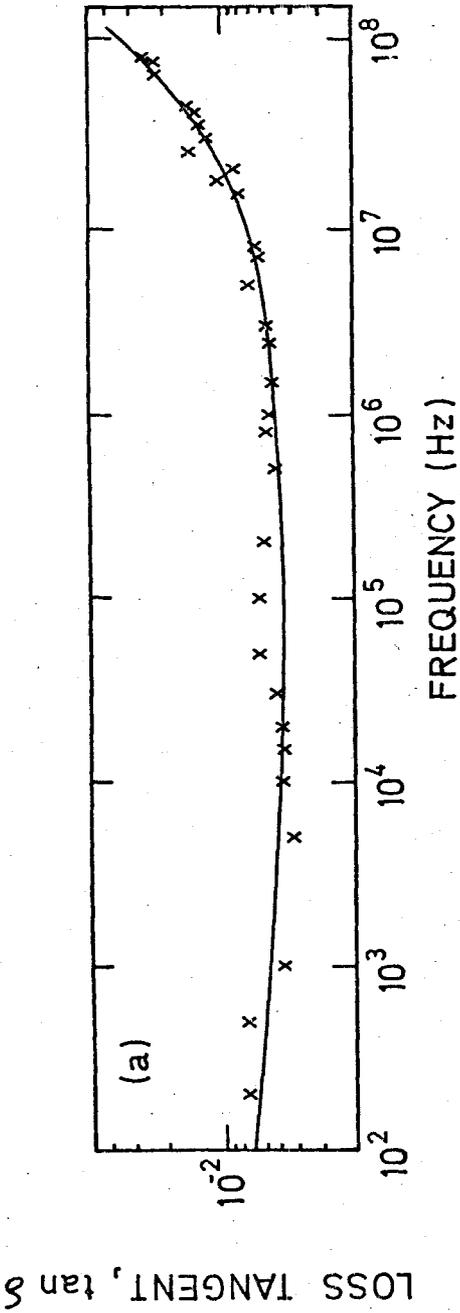but even at 1kHz and 500°C, ε' only reaches 12;   thus the change with

FIG. 6i (a) The frequency dependance of loss tangent tan δ z = 4 sialon at room temperature.

(b) The frequency dependance of the dielectric constant ϵ' for z = 4 sialon at room temperature.
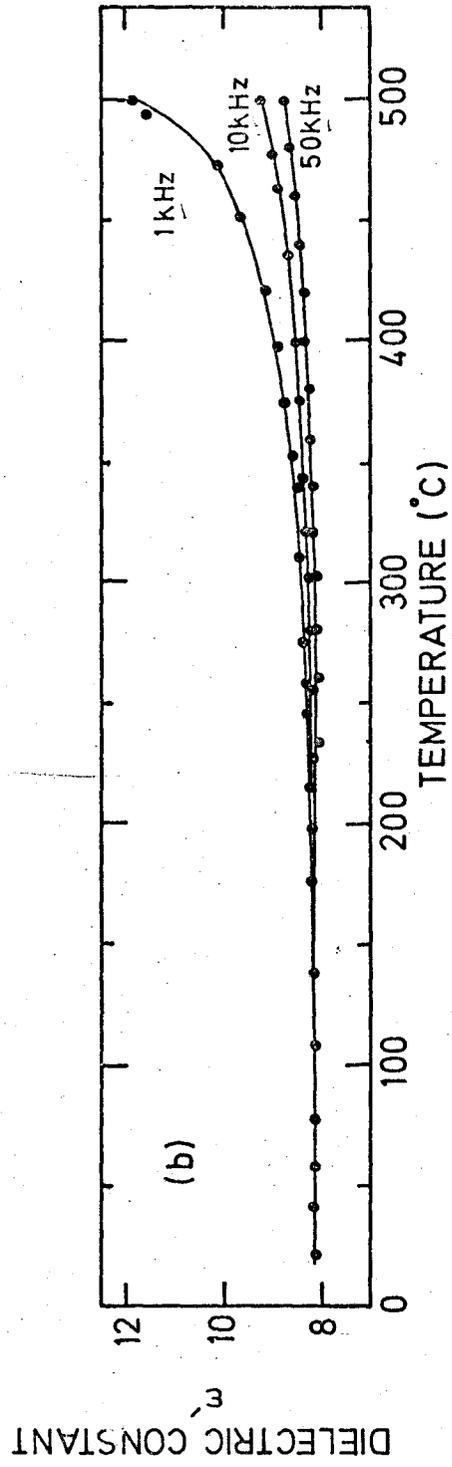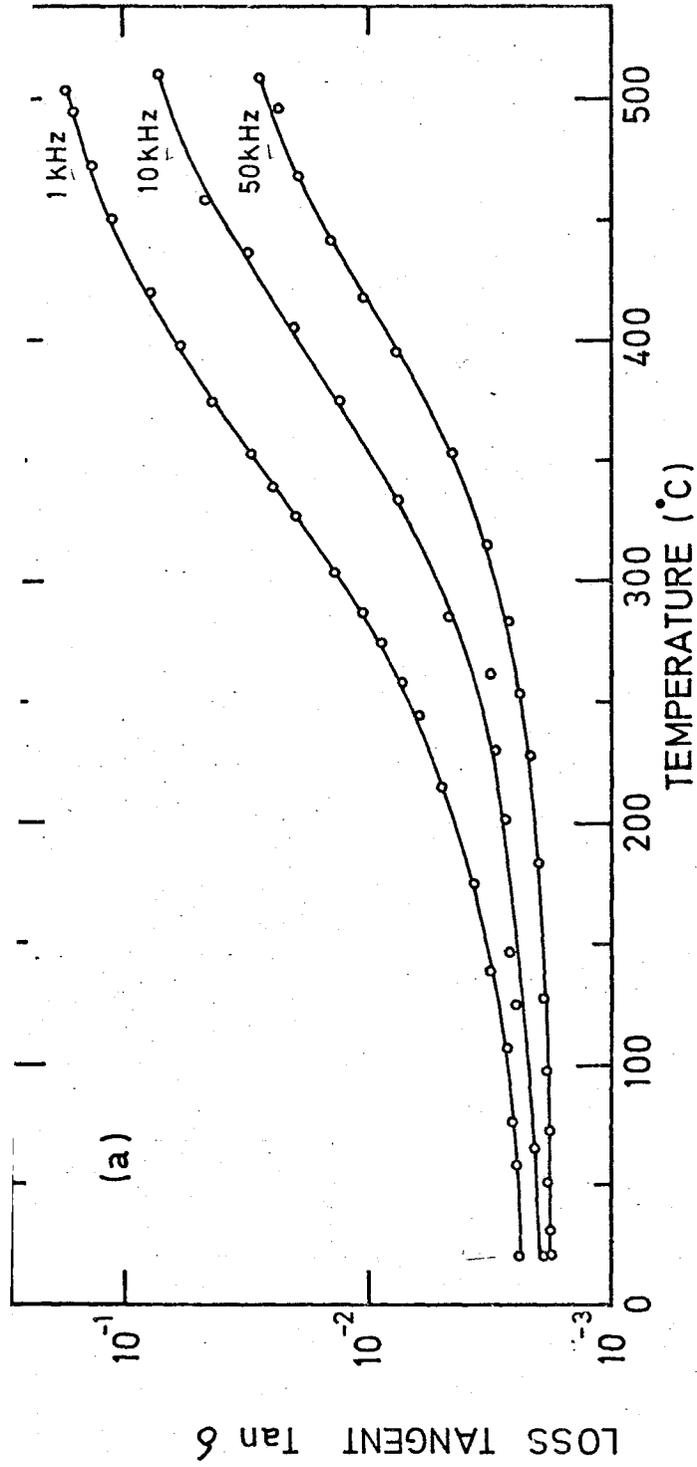
FIG. 6ii (a) Temperature variation of the loss tan. δ for z = 3·2 sialon.
(b) Temperature variation of the dielectric constant ε' for z = 3·2 sialon

temperature is small. More pronounced effects are seen on the tanδ
plot. Here the rate of rise of tanδ is fairly rapid above 300°C; again
the greatest effect occurs at the lowest frequency but it is to be noted
that the maximum value of tanδ (at 1kHz,500°C) was only 0.1. These
changes are very much smaller than those in the corresponding experi-
ments on the lithium sialons. This data on the pure sialons has not
yet been analysed in detail but it appears from qualitative inspection
that the effects are entirely in accord with the predictions of hopping
theory. In conclusion it may be noted that an independent examination
of a 30m/o Li spinel sialon was made by R.I. Sharif using the same
apparatus and technique as that with which the measurements on pure sialon
were made. The results are reproduced in Figs. 6iii and 6iv. In these
measurements a specially ground thin slice of ceramic was used. The de-
pendence of both ε' and tanδ on temperature and frequency reported in
Chapter 5 is confirmed as is also the fact that the magnitudes of the
changes are very much larger than in the pure sialon. The agreement in
tanδ values is good. The values of ε' (250 at 450°C, 200Hz) appear to be
rather lower than those obtained in Chapter 5; this is probably attribut-
able to the different specimen geometry. However, the effect of lithium
addition on the dielectric property of sialons is convincingly illustrated.

6-2 Comparison with Yttrium Sialon Glass

Some of the characteristics of the yttrium sialon glass have already
been reported. For example, Fig. 4v compared the a.c. insulation con-
ductivity of an yttrium sialon with that of a 28m/o lithium spinel sialon
and showed that the behaviour of the two materials was very similar; in
the low temperature region the results were almost identical. One
difference was revealed and seems to be associated with composition. This
is the temperature at which the exponential rise in conductivity begins.
For the 28m/o lithium spinel sialon this occurs (taking 500Hz data) at
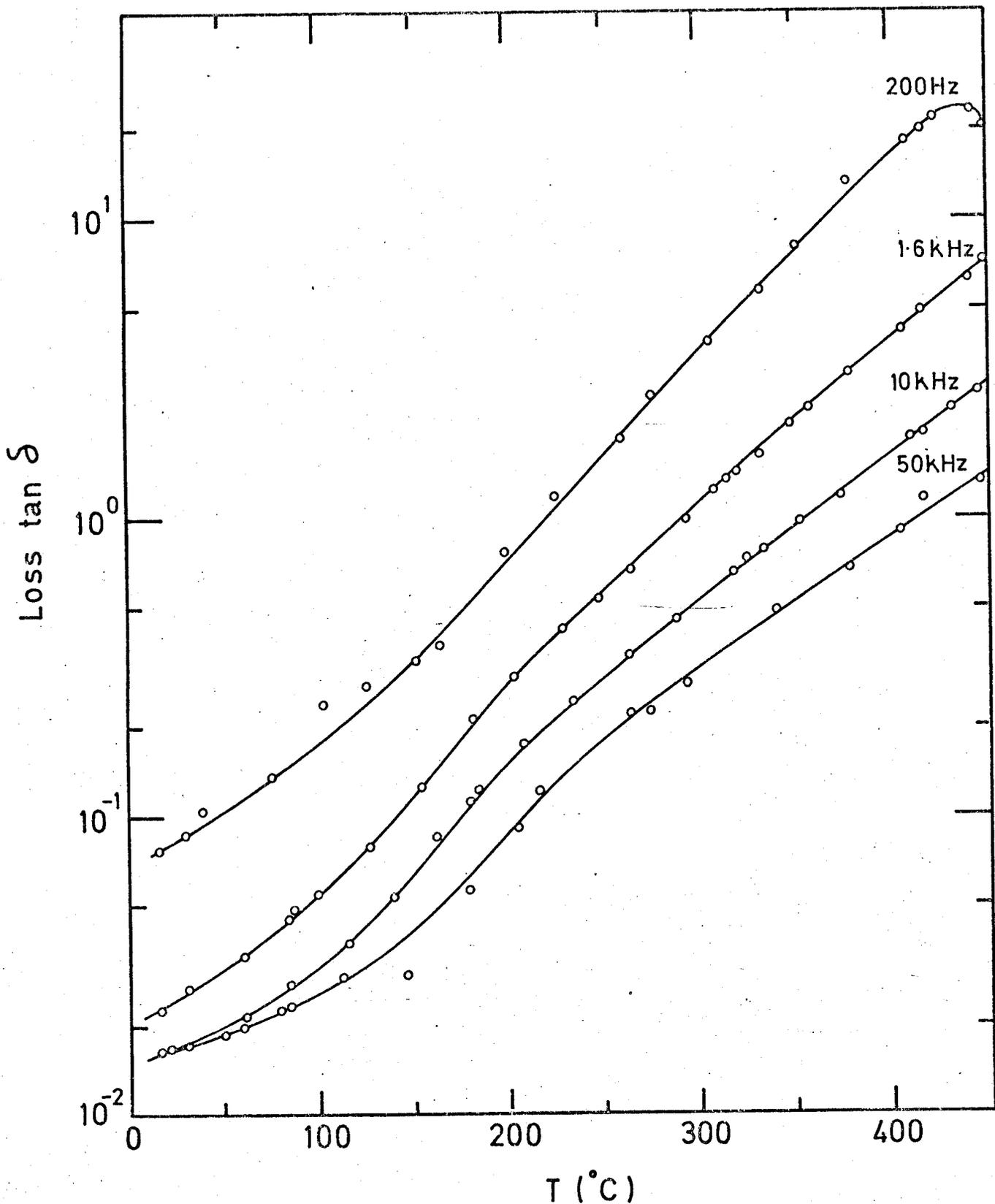230°C whereas the corresponding changeover for the yttrium sialon glass

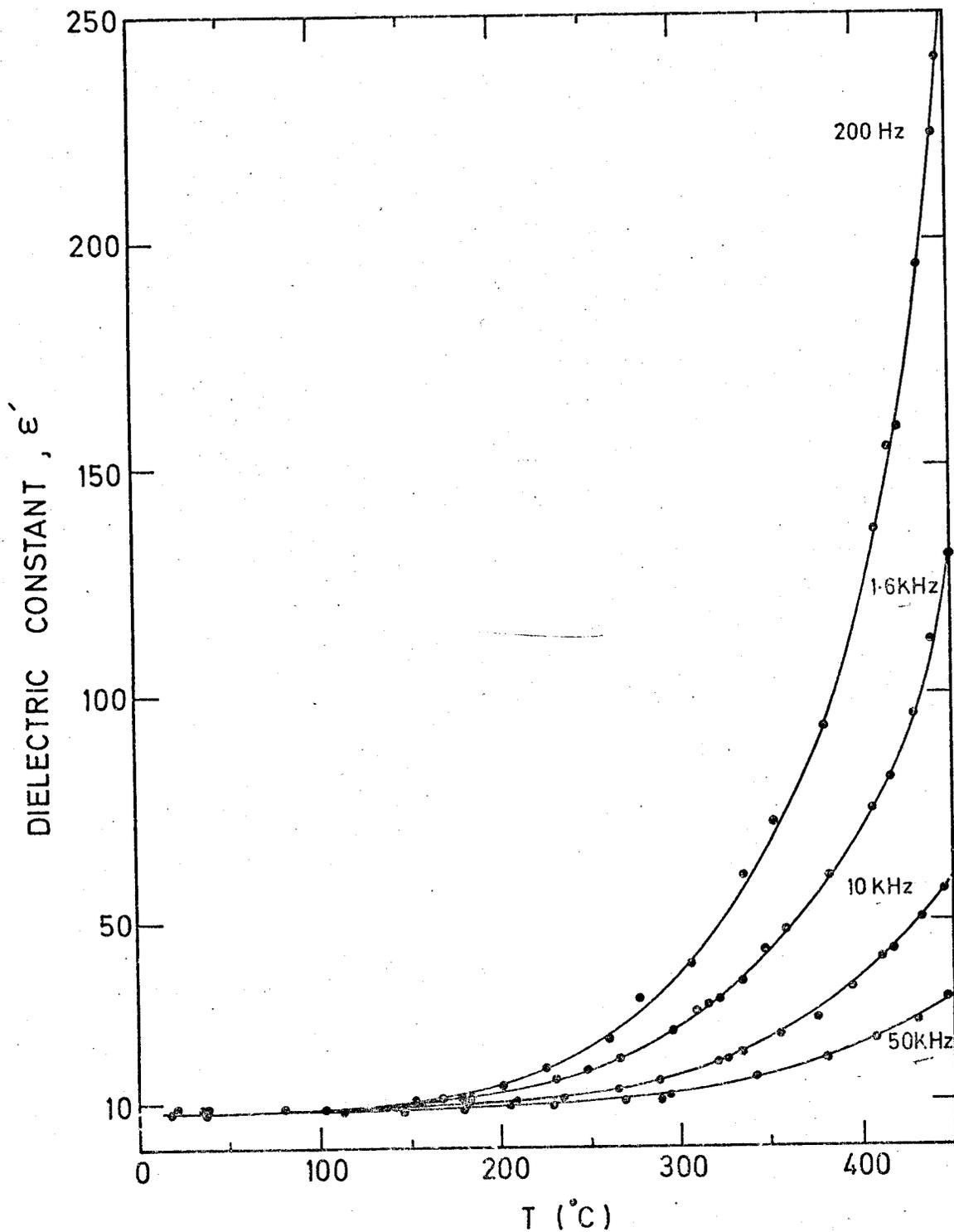FIG. 6iii Temperature dependence of the loss tangent for 30 m/o Li - sialon at various frequencies.

FIG. 6iv   Temperature   dependence   of   dielectric   constant,
ε' for   30 m/o   Li-sialon   at   different   frequencies.

takes place at a considerably higher temperature of around 550°C. It is

interesting to note that in the pure sialon the change occurs at a much

higher temperature than in either the lithium or yttrium sialons (Fig. 4vii).

Tentatively, an explanation of this may lie in the greater number of impurity

centres produced in the doped sialons which would cause multiple hopping (i.e.

the mechanism occurring in the exponential region) to be more likely at lower

temperatures. One may note also that the activation energy for the yttrium

sialon in the exponential region is 1.4eV as compared with 0.7eV for the

lithium sialon and this change can be directly attributed to the exchange

of yttrium for lithium. The similarity in the general form of the be-

haviour is particularly important as it supports the view that glassy phase

effects dominate in the sialons. Further measurements substantiating this

evidence have been made and these are briefly reviewed below.

The temperature variation of the a.c. conductivity, derived from measure-

ments on the Wayne-Kerr bridge at 1.6kHz, is shown in Fig. 6v. Although

there is as yet, not a large amount of low temperature data the exponential

region is quite well defined and the room temperature results suggests a

very marked departure from linearity in this region. The general form of

the variation is similar to that for the lithium sialons and the slope in

the exponential region yields an activation energy of 1.2eV for yttrium

sialon glass; this is in fair agreement with the previous estimate. At

room temperature the frequency dispersion of the a.c. conductivity (again

derived from bridge measurements) has been investigated in some detail.

The results are shown in Fig. 6vi. The variation of $\log\sigma_{ac}$ with frequency

is linear giving a value of s, the exponent in equation 5-2 of 0.77. This

value is almost exactly the same as that found for the lithium sialons.

Furthermore, the room temperature variations of tanδ and ε' with frequency,

Fig. 6vii, show the same trends as the lithium sialons and, taken together,

these two pieces of evidence indicate firmly that the same type of hopping

mechanism is occurring in both materials. The similarity extends also to

the high temperature region, in which a rapid rise of tanδ with temperature
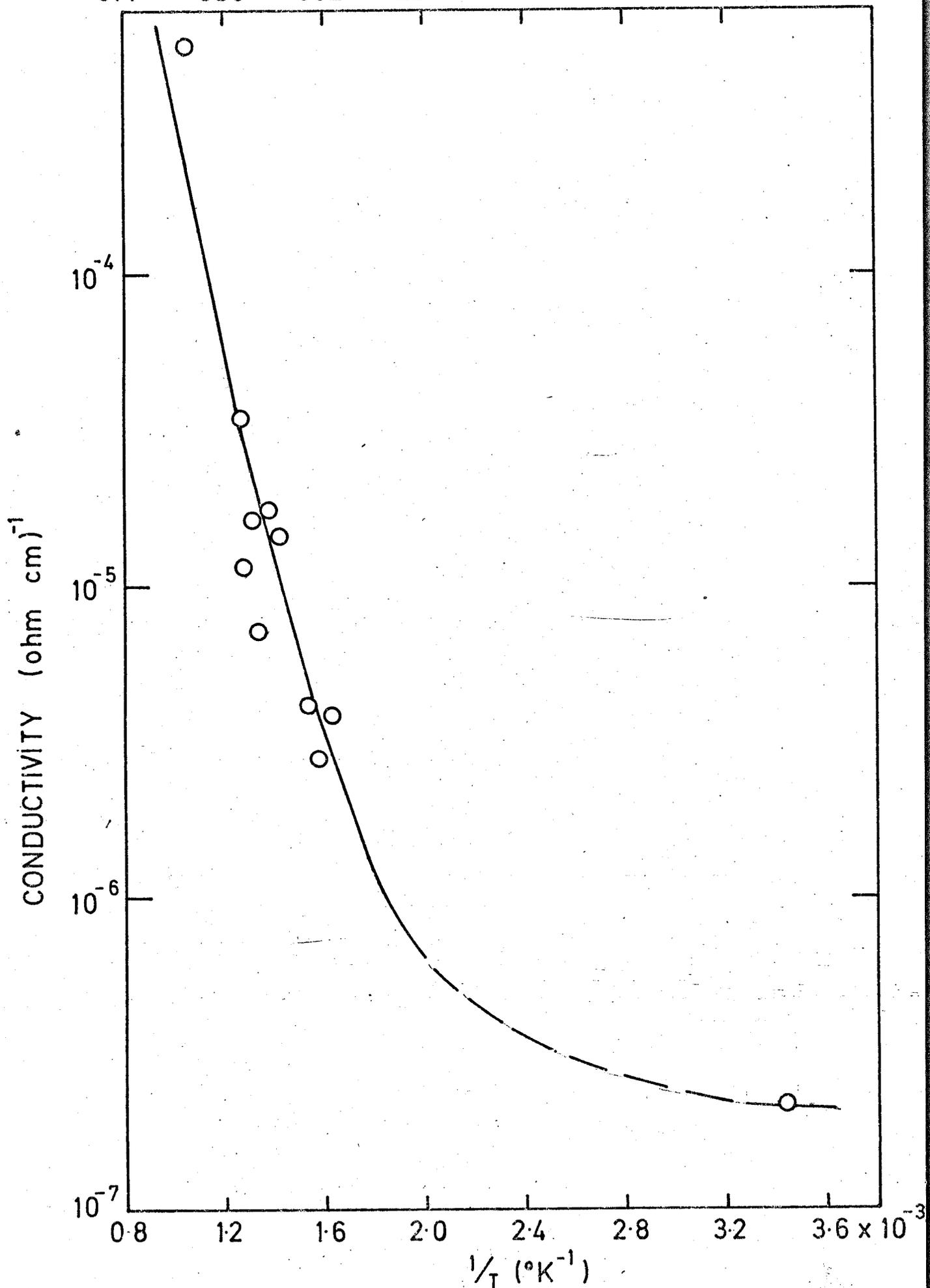
FIG. 6 v The a.c. conductivity at frequency of 1·6 kHz as a
function of temperature in yttrium sialon glass.
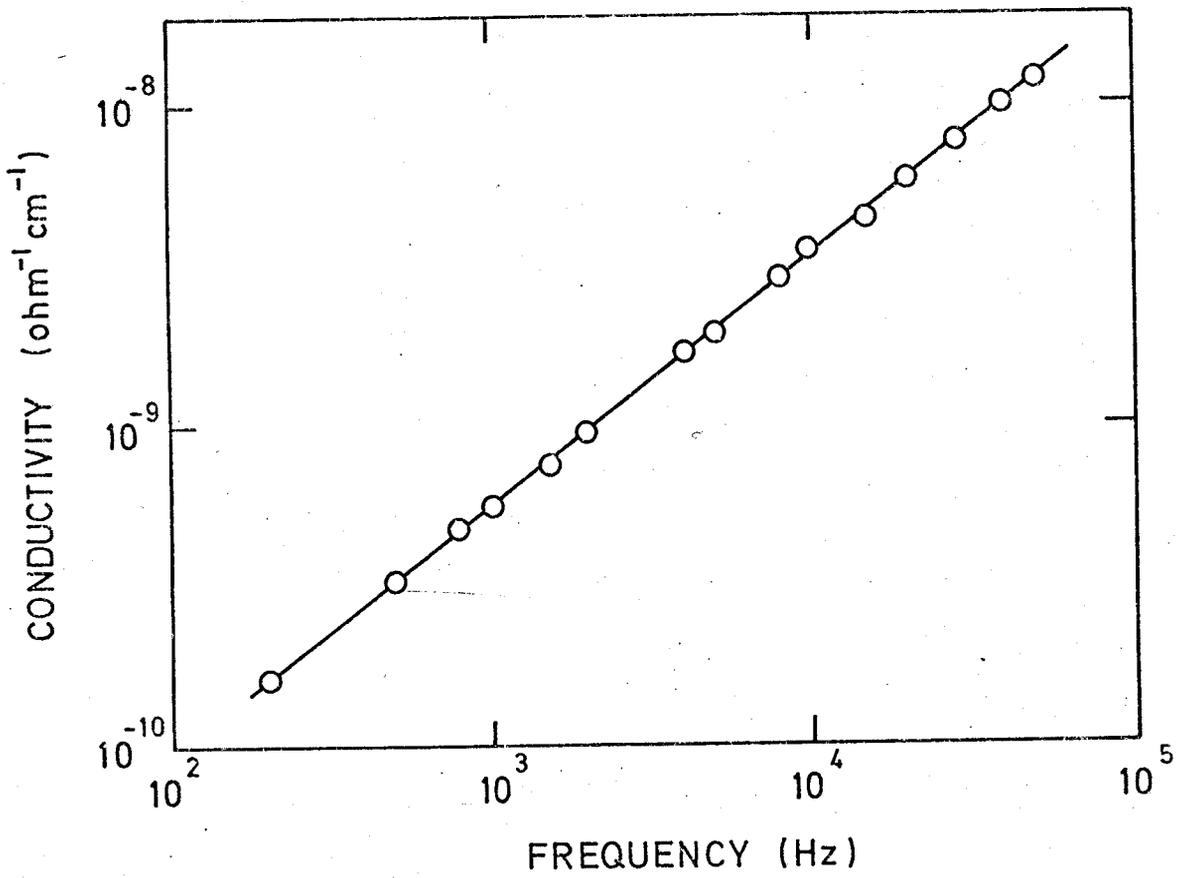
FIG. 6 vi Frequency variation of ac conductivity in
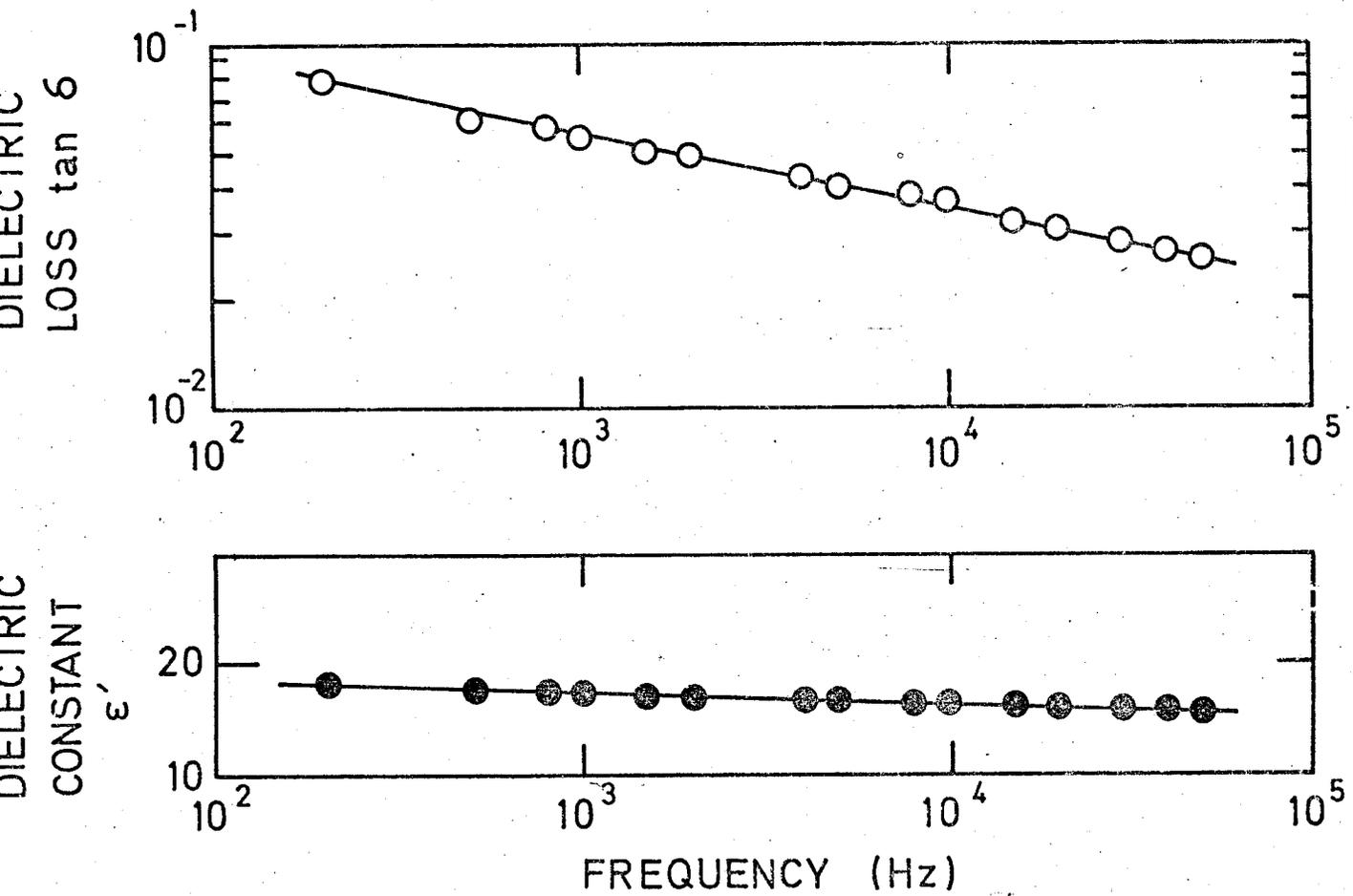yttruim sialon glass. (at room temperature)

FIG. 6 vii Room temperature frequency variation of tanδ
and ε′ for yttruim sialon glass.

has also been observed, Fig. 6viii.

6-3 Future Work

Due to their electrical degradation and higher electrical con-
ductivity there is no reason to use lithium sialons as insulating mate-
rials; pure sialons would be a far better choice.   The mechanical

properties of the lithium sialons are no better than those in the un-
doped sialons (Jama, 1975), and so there would be no advantage to be

gained in the environments in which they could be used.   Also the pure

sialons have lower values of the dielectric loss which is desirable in a

potential insulator.

For use as high temperature dielectrics the lithium sialons may have

potential since for this purpose a high dielectric constant is required

which the lithium sialons are certainly able to provide - values up to

10^4 have been recorded at a temperature of $800^{\circ}C$.

It might be possible to use the very rapid variation of the electrical

properties of the sialons in a thermometric application.   Their excellent

high temperature corrosion resistant properties may be employable so as

to give a thermometer in the range 800 to $1500^{\circ}C$, a temperature range not

very readily covered by available technology.

For all the possible uses of the sialons mentioned above more detailed

knowledge is required of the electrical properties of the new sialons, as

they are made.   The new sialon glass series have not yet been investigated.

Such a study would not only characterise the new materials but would also

be helpful in the understanding of the crystalline sialons and shed further

light on the mechanisms of conduction operating within these materials.

Studies on samples in the form of thin slices have already been started;

these will give further information in several ways.   Firstly, the different

geometry will indicate the effect of surface conduction, since the ratio of

surface to bulk material will be altered.   It will also indicate the extent

to which the geometry itself has influenced the values of the data recorded.

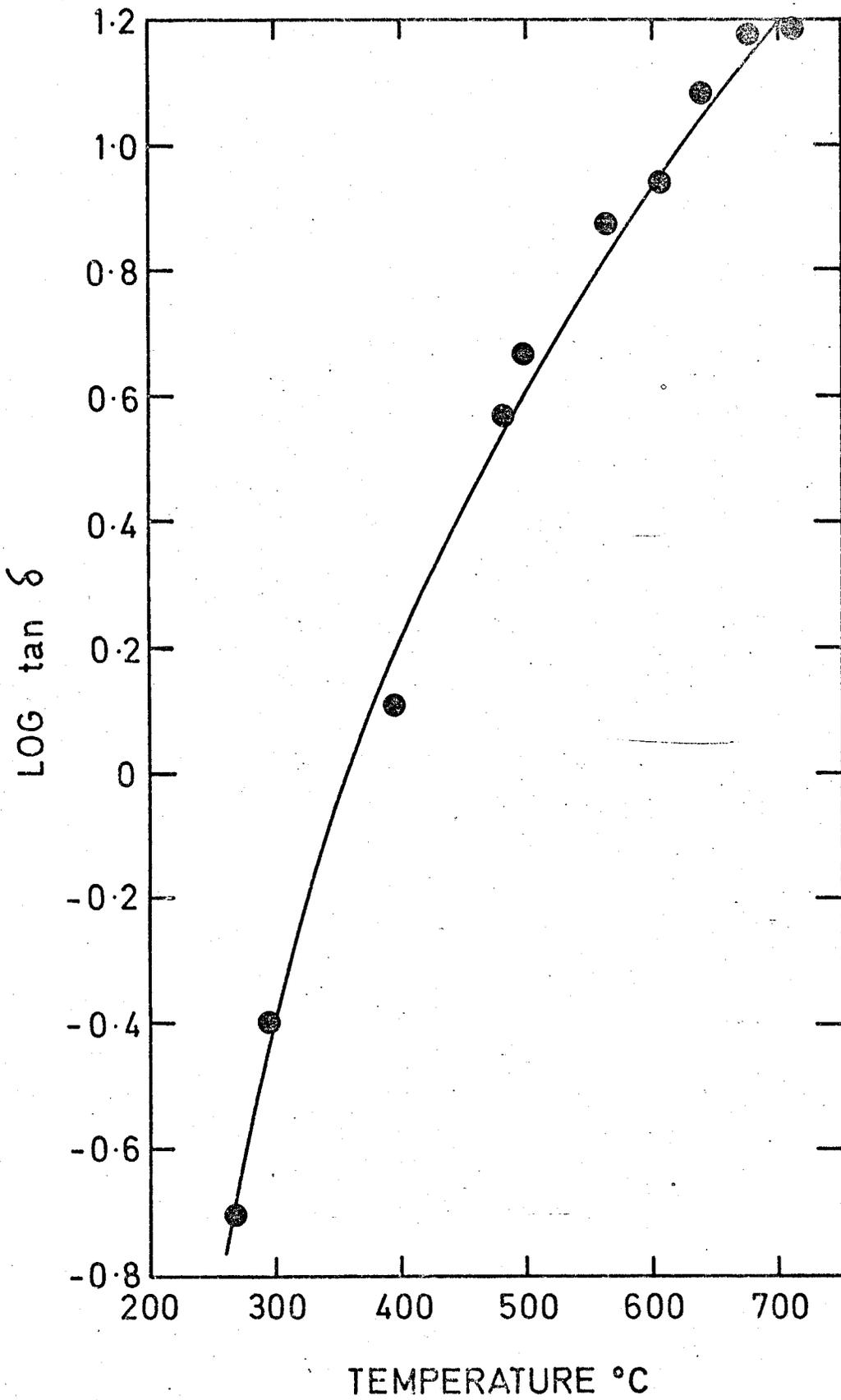The second advantage of work on thin slices is that it will allow more

FIG. 6viii Variation of dielectric loss as a function of temperature in yttrium sialon glass (frequency = 1·6 kHz)

precise determinations of the values of the sialons' properties and this
in turn will be of value in further determining the conduction mechanism.
This would be aided by more structural information on the place of the
Li^+ ion in the lattice, particularly whether it goes into the glassy phase
or into the β' crystallites.   The present work suggests, but is in no way
conclusive, that the lithium is in the glassy content.   Indeed the glassy
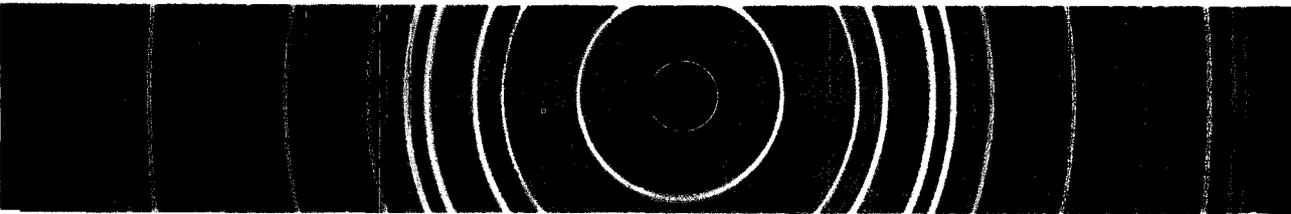content is itself very interesting and warrants further work.

APPENDIX 1 X-ray powder photographs of

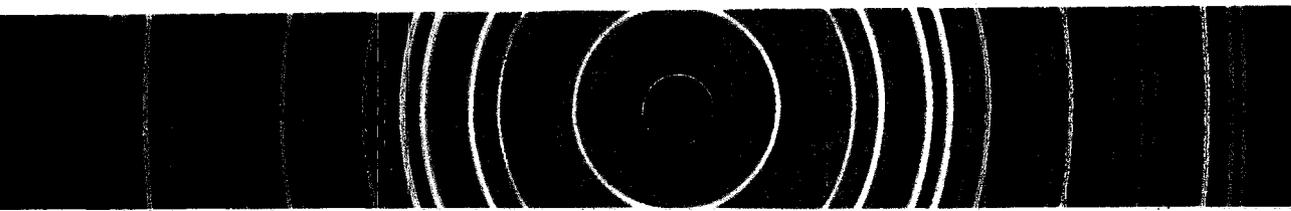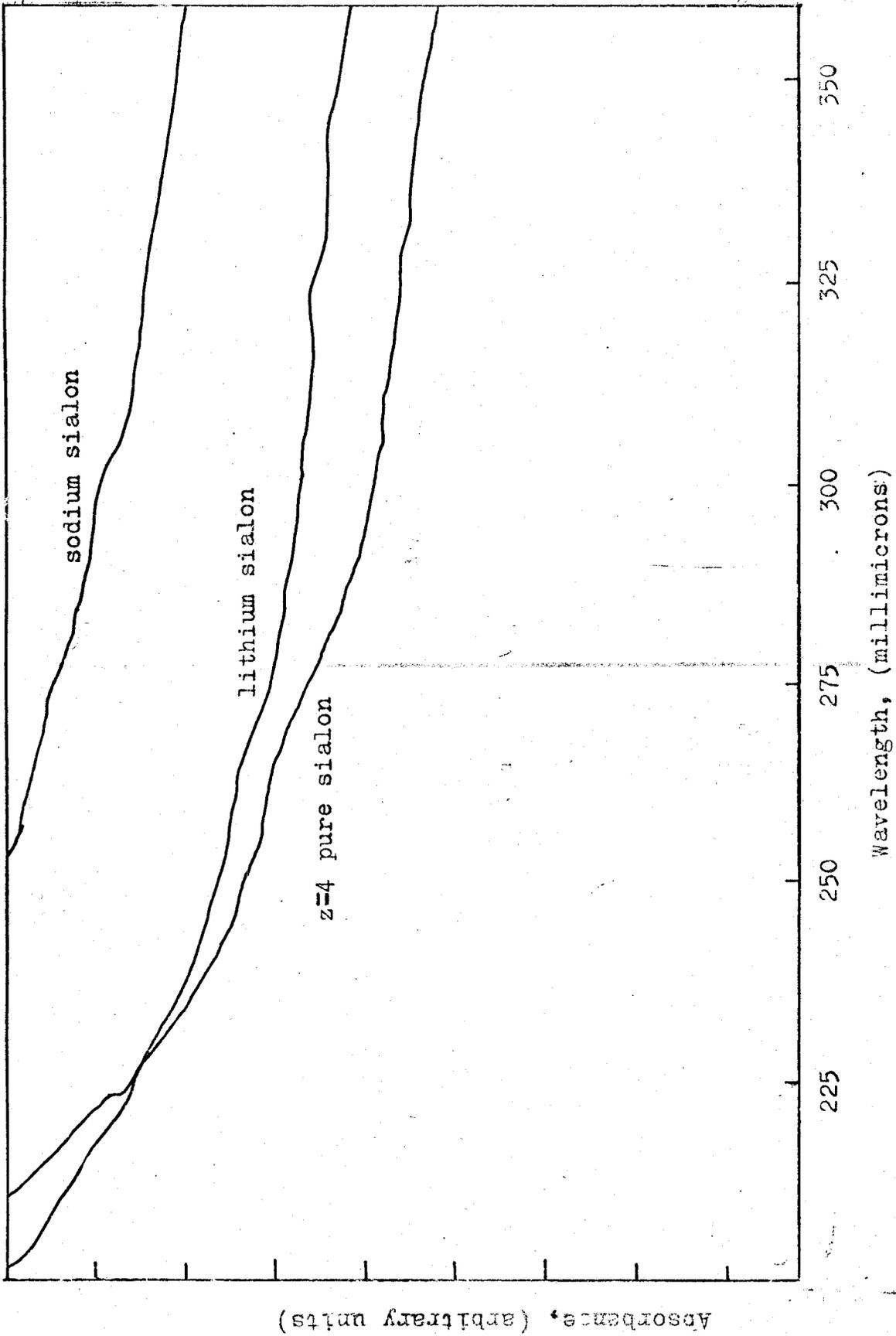a lithium sialon before and after electrolysis
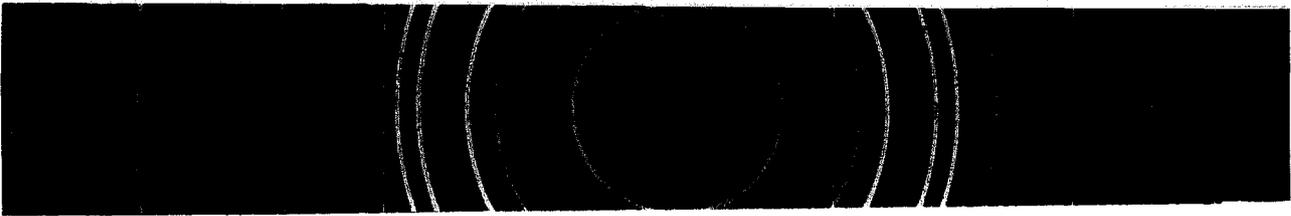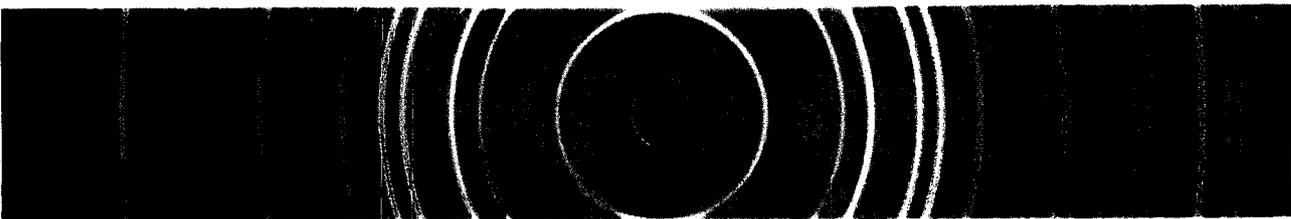
A - Before electrolysis   B - End connected
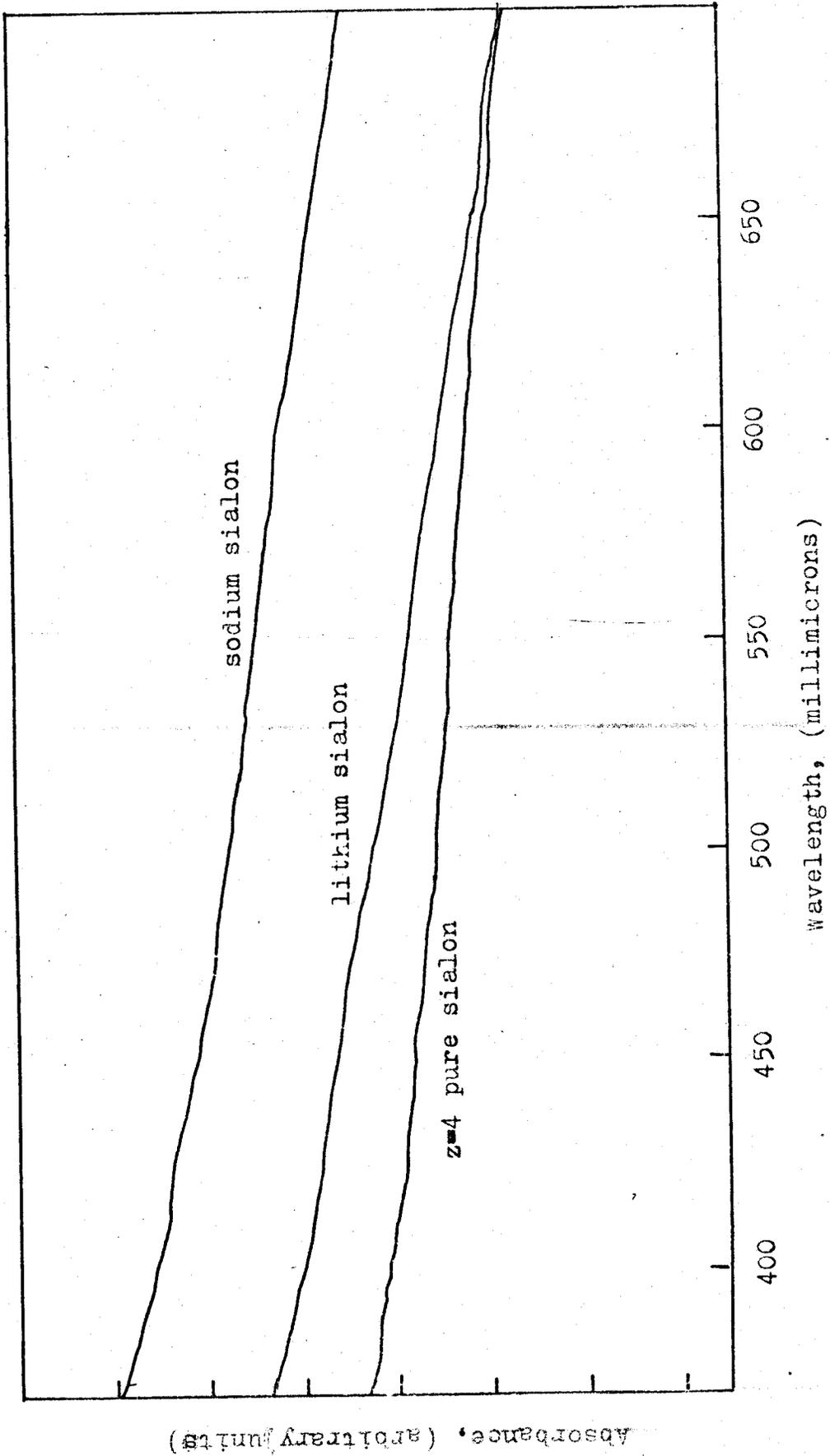   to positive terminal)
)
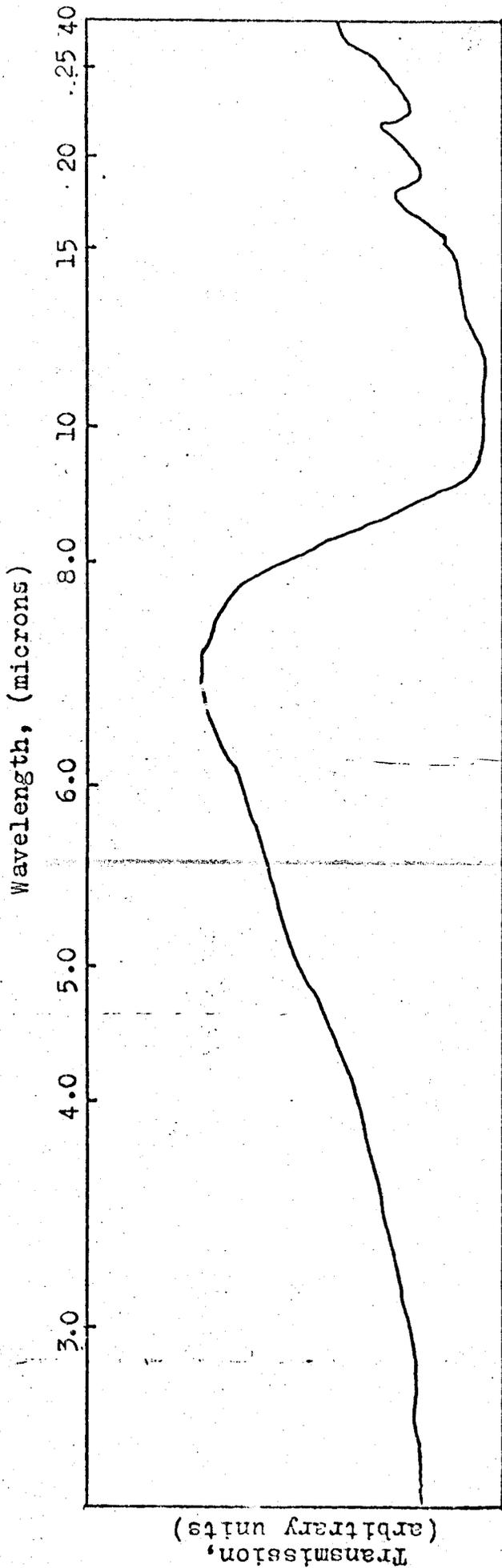   )
                           C - Centre of sample   )   After
) electrolysis
)
                           D - End connected   )
                                to negative terminal)

APPENDIX 2 Optical spectra of a pure, a lithium and a sodium sialon

sodium sialon

lithium sialon

z=4 pure sialon

wavelength, (millimicrons)

absorbance, (arbitrary units)

APPENDIX 2(cont.) Optical spectra of a pure, a lithium and a sodium sialon

APPENDIX 2(cont.) Transmission spectrum of 30m/o lithium spinel sialon

REFERENCES

Arrol, W.J. 1973 2nd Army Mater.Technol.Conf. Hyannis,
   Mass. USA 13th-16th Nov.

Austin, I.G. and Mott, N.F. 1969 Advances in Physics 18
   no 71 p41

Buckley, H. and Sharif, R.I. Private communication

Davis, E.A. and Shaw, R.F. 1970 J. Non Crystalline Solids
   2 pp406-431

Kingery, W.D. 1960 Introduction to Ceramics

Jack, K.H. 1976 J. Mater.Sci. 11 pp1135-1158

Jama, S.A.B. 1975 Ph.D. thesis University of Newcastle

Mott, N.F. and Davis, E.A. 1968 Phil.Mag. 17 p1269

Thorp, J.S. and Sharif, R.I. 1976 J.Mater.Sci. 11 pp1494-1500.